Date: 24/10/25

On a Decelerated Universe

An Orientation Guide

Oliver Rast, Private Research Facility, Bonn (Germany)
Email: decelerated.universe@posteo.de

*'Eine Gesellschaft, die meint, den Anfang der Welt mit einem Knall erklären zu können, sagt mehr über sich aus und weniger über die Welt.' Weizsäcker, C. F.**

Abstract

The specialised field of extragalactic cosmology is about one hundred years old. Over the time, it is divided into many sections. A new framework is needed to overcome the severe difficulties of the standard model of cosmology. In this model, the period of evolution of the universe is set to 13.8 Billion years. The initial limit is a primordial fireball (Big Bang) and a continuous expansion of the whole matter. To fit the observations to the model, many additional assumptions are needed, such as inflation, dark matter, and dark energy. To date, these assumptions can not be confirmed or refuted. Meanwhile, the community of cosmologists can provide no observations that could falsify this **standard model of cosmology**.
This paper demonstrates a spheric universe of constant size and content of matter-energy. This model is close to Einstein's first ideas in his cosmological considerations. The misapprehension was to call such universe a 'static universe'. Contrary to this my universe is very dynamic.
I name it '**Schwarzschild universe**', because Karl Schwarzschild demonstrated 1916 that huge amount of matter form robust spheres.
In this paper I will bring together discussions and hypothesis before 1933 of Albert Einstein, Karl Schwarzschild, Arthur S. Eddington and others, and observations after 1945. I will submit proposals to avoid additional assumptions or 'new physics'.

* 'A society that opines the beginning of the world (i.e. the universe) was a (Big) Bang, says more about itself, and less about the world.'

Table of Content

1 Introduction: The Schwarzschild Universe

According to experience aggregations of matter tend to arrange to spheres by gravitational forces, (i.e. they become celestial bodies). Even small fractional amounts of the mass of our earth arrange to compact spheroids. Aggregations larger then 8% of the sun's mass ($0.08\,M_{\odot}$) have the capability to ignite nuclear fusion, in case there is sufficient hydrogen as nuclear fuel. Due to the energy flux, celestial bodies even heavier than 1.4 $M_{\odot}$ cannot shrink to their Schwarzschild radius for a long time. Even clusters of stars or clusters of galaxies tend to group to spherical formations. **Why shouldn't the whole universe arrange to a sphere or haven't had this shape just 'everlasting'??**

The thesis of this paper implies that all Schwarzschild objects we usually denominate 'Black Holes', extrinsic look like three dimensional dark spheres. Intrinsically they enclose their mass-energy in a 4-dimensional space-time. Everything happens upon their
3- dimensional 'surfaces'. The biggest Schwarzschild object we can observe, is the universe on the whole. All processes happen upon i.e. inside its surface.

Along the lines of moons and planets, the objects and creatures have not the capability to leave offhand their 2-dimensional surface into the outer space. **But they can't sink to the centre of these firm celestial bodies as well.** Similar to this, the outer and inner region of the 4-dimensional sphere of the cosmos is not accessible. But we can determinate the capacity of the 3-dimensional surface. For a long time we have sufficient data of observations to revise the standard model of cosmology.

2 Properties of a Schwarzschild Universe

Table 1: Comparison of the Standard model and Schwarzschild universe

Standard model	**Schwarzschild universe**
Big Bang: The cosmic microwave background (CMB) considered to be the redshifted image (z~1100) of the 3000 Kelvin plasma independent from the observer's location all over the cosmos.	**No Big Bang:** The CMB is the luminous glare of our own proto galaxy (z~534). Its light circled the universe completely. Its intensity is strongly dependent from the observer's position (chapter 2.1).
Inflation means matter out of nothingness ('primordial atom'). A particular size of the cosmos is reached instantaneous.	**No inflation:** A fixed amount of matter exists in perpetuity. Size and mass-energy is always constant (chapter 2.2).
The **Expansion (of the space)** produces the redshift of light, similar to the Doppler effect, and causes time dilation and dilution of photons.	**No Expansion:** Photons and also moving elementary particles are loosing energy, affected by gravitational waves. No time dilation and dilution (chapter 2.3).

Standard model	**Schwarzschild universe**
The **Cosmological constant λ** causes a force of expansion, which puffs out the cosmos. Curvature of space can be neglected nowadays.	**Curvature of space:** Einstein postulated a constant figure λ. In the Schwarzschild universe, it is relevant dimension for the curvature of space (chapter 2.4).
Dark matter can not interact with photons. It explains the anomalies of motion of galaxies and hot gases. It provides an efficient building of structure at the early cosmos.	**Dark <u>baryonic</u> matter:** Ordinary elementary particles that are not affected by any electromagnetic radiation, because there are no photons at all in the early stages of the universe (chapter 2.5).
Dark energy: Accelerated expansion of space due to a 'repulsive force'.	**No dark energy:** No expansion at all. So dark energy is not necessary (chapter 2.6).
Cosmological Principle: An idealised homogeneous and isotropic universe. The real universe has to be averaged over distances about 100 Mpc.	**Homogeneity and Isotropy:** It was the early state of the universe an ideal way. The evolution increases more and more the inhomogeneity (chapter 2.7).
Primordial Fluctuations: The observations by the James Webb Telescope suggest a complete structure building already 200 million years after Big Bang.	**Just Quantum Fluctuations:** There were trillions of years to form the cold and homogenous hydrogen to voids and filaments. Not till then small celestial bodies with the capability to nuclear fusion arose (chapter 2.8).
Primordial Nucleosynthesis: The mass ratio H:He ought to be 3:1 just before the recombination era.	**Only Hydrogen at the Beginning:** Helium and somewhat lithium is brooded by brown dwarfs gradually (chapter 2.9).
Initial Mass Function: A wide range of stars ($0.1\,M_\odot$ to $> 10\,M_\odot$) and even Black Holes should emerge instantly after Big Bang.	**Continuous Aggregation:** A development of small hydrogen 'planets' to giants of some $10\,M_\odot$ over a period of many 100 billion years (chapter 2.10).
The Hubble Radius increased from the beginning. Tentatively it has stopped nowadays.	The **Schwarzschild Radius** is identical with the contemporary Hubble Radius H_0. It determines all other measurements of the cosmos (chapter 2.11).
Critical Density: The density of matter determines the further evolution of the cosmos: Shrinking, expansion or equilibrium state.	The **Average Density** is not critical. It is determined by Schwarzschild's equation (chapter 2.12).

2.1 Big Bang/ Cosmic Microwave Background

1948 it was widely accepted that the cosmological redshift of light is due to an expansion of space. At that time one could observe redshifts of galaxies up to 0.2. Gamov grossed up the effect of redshift ad infinitum. He concluded the former state of the universe to be much denser and hotter. He denominated this state a '**primordial fireball**' (→ Gamow 1948). Hubble's doubts concerning the 'reality of expansion' of the whole world were commonly neglected (→ Hubble 1953).
Finely it was common sense that the cosmic microwave background (CMB), measured for the first time by(→ Penzias & Wilson 1965), was the image of this fireball. According to that, the surface of the expanding and cooling fireball became visible at a temperature of 3000K by recombination of the plasma. Redshifted to 1100, one can observe a background radiation of 2.73K all over the sky.

My thesis:
The consistent application of the general theory of relativity was neglected. Redshift without Doppler effect or expansion of space was entitled 'gravitational friction' or 'tired light'. But cosmological redshift of every single photon is induced by loss of gravitational waves.
In the **Schwarzschild universe**, the **cosmic microwave background** (CMB) is the z~534 redshifted image of ~1460K warm matter. It is provided by primary brown dwarfs, which had been the edge of evolution 88 billion years ago. At that time, they had congregated amongst planets at the same place of our galaxy to date. I will denominate this location the **'self-pole'** of our place in the universe. Even observers on far-off galaxies have their own self-pole and could observe a CMB. In contrast to the CMB of the standard model, observers in voids see much less proximate galaxies and no CMB at all.

2.2 Inflation

Making a rough estimate to inflate the 'primordial atom' to the size of the cosmos to date during 14 billion years: The linear physical size of the standard universe has been increased more than 1000 times since the recombination era at z~1100. That means round about 10 times duplication with corresponding cooling down. To get the radius of the cosmos to date out of the size of a hydrogen atom ($a_0 \sim 5.3 \cdot 10^{-11} m$ = Bohr's radius), one must redouble its size more than 120 times $2^{121} \sim 10^{36}$, during the corresponding time of ~ 14 billion (light) years.
But according to the tale of inflation, the size of the primordial atom means Planck's length, that is $l_p = 1.6 \cdot 10^{-35} m$! To receive only the Bohr's radius a_0 out of Planck's length, one needs more than 80 further reduplications. The theoretical physicist Alan Guth makes up the story of the '**inflationary universe**' (→ Guth 1981). Hence he hides an almost infinite time interval ($t \sim 10^{68}$ years) in a non observable small period of time and dimension, compared to the 'final' 10 times of reduplication ($14 \cdot 10^9$ years). The matter of the universe is generated ('inflated') out of nothing!

My thesis:
There is an everlasting fixed amount of mass-energy ($E \sim 8 \cdot 10^{69} J$) in the **Schwarzschild universe**. There is a continuous evolution of stationary single hydrogen atoms, to generate more and more kinetic energy, photons, and heavier elements. The initial state of the Schwarzschild universe is not further explainable, just like the 'primordial atom' of the standard model.
*The ancestral cloud of hydrogen is in the truest sense of the word the **causation** of everything. There was and there is even not '**nothing**'.*

2.3 Expansion of the Cosmos

Physicists saw in a 'static' universe not only an universe that has a constant size, but also has an unchanging state of evolution. Thus holding the balance, there must be provided new matter perpetually. Eddington conceives Einstein's spherical universe to be unstable (⟶ Eddington 1930). After Edwin Hubble detected the redshift of light, the idea arose of the continuing expanse of space. Initially scientist expected that the enduring deceleration of the expansion by gravitational forces stagnates nowadays. Anyway, this was the expectation until the 'detection' of dark energy (refer to chapter 2.6).

My thesis:
The spherical universe of constant mass-energy is stable and don't collapse. Its radius R, and thus Einstein's originally λ, is an important and constant quantity.
It can be determined by the available data of observations to date .
To describe the spherical universe to be static is incomplete, just as to describe the geologic history of the earth without continental drift, earthquakes, and vulcanism. Even against the background that the radius and the mass of the earth has been practically constant over many billion years.

2.4 Cosmological Constant

Albert Einstein introduced within the scope of a finite closed universe his cosmological constant $\lambda = 1/R^2$ (⟶ Einstein 1917). He thought it to be dispensable after Edwin Hubble's detection of the universal redshift of extragalactic objects. Soon it became common sense that the redshift is caused by an escape movement (radial velocity) of far-off galaxies. In the early 2000th, 'Lambda' (Λ) got a new meaning, because data of supernovae suggested that the universe expands faster again in recent time. (refer to chapter 2.6, 'Dark Energy' and chapter 6.4, 'Supernovae').

My thesis:
Einstein had missed to apply his theory of gravitational waves to elementary particles, atoms, and photons.
Otherwise he had have the possibility to ascribe energy-losses (i.e. redshift) to photons by irradiation of gravitational waves. Thus he could have defended his 'static' universe with a constant radius $R=\lambda^{-1/2}$.

2.5 Dark (baryonic) Matter

At the **standard model** according to an overview of (⟶ Groom & Scott 2019), only 4.9% of the matter is observable baryonic matter. This model is also denominated **LambdaCDM**. The Greek capital letter 'lambda' = Λ represents '**dark energy**' (68.6%) and CDM represents **'cold dark matter'** (26.5%). Dark matter has the feature not to interact with photons, but exclusively to become noticeable by gravitation. It plays an important role to explain the deviations of motion from Newton's principles at cosmic scales.
At the beginning of the cosmic evolution, dark matter is necessary for structure building. Otherwise the homogeneous baryonic matter could not agglutinate under the immense inrush of photons of the **primordial fireball**. On the other hand, one has to explain the nearly constant rotational speed of the outer sections of spiral galaxies. Furthermore, the to high velocities of ions in very hot plasma clouds in elliptical galaxies is not explainable without dark matter; hence the ultra hot plasma should have left the galaxies due to low gravitational forces, just as well the too fast galaxies in galaxy clusters.

My thesis:
Not only matter that is to a certain extend immune against impacts of photons could be named 'cold dark matter', but also conventional baryonic matter in the form of hydrogen atoms that is not exposed electromagnetic radiation at all. By undertaking a backward projection of the evolution of the **Schwarzschild universe** to the non observable pre-fusion-era, one can calculate that was the case.

Already (⟶ Zwicky 1937) noticed that one can not reconcile the observed mass of the Coma cluster with its mass, estimated by the peculiar velocities of the single galaxies. If one applies Newton's law of gravitation, this galaxy cluster should had dispersed long ago due to the galaxies' high velocities. Therefore Zwicky postulated a huge amount of dark matter to get a sufficient escape velocity. This matter should not to be detectable with the earthbound technology of that time, owing to a very small ratio of mass to luminosity or to a non-visual spectral range.
By means of the enormous technical progress, all hopes were balked to detect dark matter. Even the method of 'pixel lensing', an effect of gravitational lensing, revealed a much too less amount of unimposing matter to get the high contingent of dark matter, needed to explain

Zwicky's observations (refer for instance to → Cardone & Cantiello 2003). Also with the aid of particle physics, there was found no candidate for dark matter, although searching for decades.

My thesis:
Zwicky and his contemporaries could hope, the 'missing mass' in galaxy clusters to be common baryonic matter. This matter should have been revealed by improved observation technologies. This couldn't be affirmed until to date. Dark matter soon celebrates its 100. birthday, without any evidence of its existence. *One should better admit, not understanding the geometry of the cosmos and its influence on Einstein's kinetic laws.*

2.6 Dark Energy

(→ Perlmutter et al. 1998) looked back on long lasting observations at their 'Supernova Cosmology Project'. They gauged the light curves of 42 supernovae type 1a (SNe1a).
They are regarded as 'standard candles' to determine the size of the cosmos. Actually they wanted to identify the **deceleration** of the space expansion by gravitational forces, but instead of this, they found that there must be an **acceleration** at redshifts lower than 0.73.
Michael S. (→ Turner 1999) invented a kind of 'negative gravitation' to provoke this acceleration: '**dark energy.**' Till this day, scientists have no idea of the physical mechanism of this interpretation.

My thesis:
The cosmological redshift is due to gravitational energy-losses of single photons. One needs no space expansion at all. The expected relation of redshift to distance in the **Schwarzschild model** is a falling exponential function. One can also find it at every reduction of electro-magnetic or radioactive energy. In standard cosmology, it fakes an accelerated expansion. To convert this error, one has to compare the comoving distance D_{com} of the standard model with the logarithmic distance $D_{\log}$ (equation 10) of the Schwarzschild model.

2.7 The Cosmological Principle

Cosmologists make statements about homogeneity (uniformity) and isotropy (directional independence) of the cosmos. Assuming the outer space to be perfectly homogenous and isotropic, the cloudless night sky looked like an uniformly gleaming fog zone. Instead of this, one see structures: Stars, nebulae, and the belt of the Milky Way. The cosmological principle implies that the universe is homogen and isotropic, averaged at large scales (~100 Mpc) (refer to Schneider 2008, page 145 and page 277ff.). It also serves as a simplification of the equations of the General Theory of Relativity at large scales.

My thesis:
The primitive state of the **Schwarzschild universe** fulfils the cosmological principle in an ideal way: The atomic material is located in uniform distribution and motionless on a 3-dimensional sphere. After many trillion years, it became the to date well-established spongy structure called voids and filaments, but without any celestial bodies or photons. The further development is comparatively short and took a few 100 billion years, and one can observe the last 88 billion years. At that time, photons, planets, stars, clusters, and galaxies were arising. The cosmological principle is being ruptured with an increasing rate (refer to also chapter 2.10 and 6.1).
Thus the Schwarzschild universe is *not* static and *not* unstable, despite of constant dimensions.

2.8 Fluctuations

According to the **standard model**, all structures of the universe should have constituted from the almost homogen primordial fireball in a very short while, compared to the fixed evolution time of about 13.8 billion years. The shortage of time becomes more and more urgent with every technical progress: **Primordial fluctuations or perturbations** ought to explain the fast structure formation (→Linde 1995). The James Webb Space Telescope (JWST) has the capability to observe structures only '200 million years after big bang', i.e. objects with a redshift of $z \sim 19$. There one can obviously see complete galaxies!

My thesis:
$z \sim 19$ represents a distance of $D_{\log} \sim 42\,Glyr$ in the **Schwarzschild universe**; these objects are only $2\,Glyr$ away from luminous and ultra-luminous infrared galaxies (refer to chapter 6.2.1 ff.) near the **opposite pole**. Even these galaxies have had a further evolution of $44\,Glyr$, starting on the location of the 'microwave background', in this paper named '**self-pole**' (chapter 3.2). One can explain the continuous and slow evolution, building all structures like stars, galaxies, and black holes much more plausible in the Schwarzschild universe, compared to the pandemonium in the standard model.

2.9 Composition of the Schwarzschild Universe

The **standard model** implies a **primordial nucleosynthesis** a few minutes after the Big Bang (BBN = Big Bang nucleosynthesis). It generates a mass ratio of hydrogen to helium of 3 to 1 and a little lithium (→Schneider 2008, page 163ff).

My thesis:
At the beginning of the **Schwarzschild universe**, one must not postulate a mix of different chemical elements. The ratio of hydrogen to helium, one can observe today, was

bred from origin **brown dwarfs**. They could be named 'population IV stars'. Their nuclear fire can expire in between, until they merge to heavier stars to flare up again. These stars (red dwarfs) are the population III stars, predicted by the standard model, but not being observed nowadays. The direct fusion of two or more celestial bodies is a more important process in the evolution of the Schwarzschild universe than at the standard model.

2.10 Population Synthesis

The initial composition and the chronological evolution of star clusters and galaxies is the topic of population synthesis; refer to (→Schneider 2008, page 132ff).
Due to different lifetimes and spectra of star populations, one can see very variable overall spectra of galaxies over billion of years. At the **standard model**, it is supposed that galaxies occur with high amount of UV radiation soon after recombination. This radiation decays very fast. Therefore, one has to assume an initial mass function (IMF) with a high fraction of massive stars that appear 'immediately' after Big Bang. Even initial black holes are postulated for that time. These spectra became redder and infra-redder with declining overall luminosity (colour evolution of spectra).

My thesis:
In the **Schwarzschild universe**, the evolution of star populations is just reverse to the **standard model**. There had been a development of several 100 billion years, before brown dwarfs arose, as described in chapter 2.9. In that long period, there was no nuclear fusion, and only jupiter-like 'planets' of pure hydrogen populated the universe. They also built planet clusters. About 88 billion years ago, i.e. around the self-pole of the cosmos, there had been populations of stars with an effective temperature of about 1460K, outshining the leaving Jupiter-objects.
The further colour evolution was leading to more and more brighter and bluer galaxy-spectra, not least due to a increasing amount of Active Galaxy Nuclei (AGN). I estimate that this cosmological development is not at a turning point to date.

The sun harbours over 90% of all known chemical elements. Nonetheless the sun's spectrum is rather close to Planck's spectrum. In contrast, the spectra of *modern* T-dwarfs are totally bumpy. One has to struggle to determine the effective temperature T_{eff} of these stars. The surface temperature of the sun is $T_{eff} \sim 5700\,K$; all atoms are existing as plasma. They provoke only narrow absorption lines. But a modern brown dwarf's atmosphere ($T_{eff} \sim 1460\,K$) has a lot of organic molecules to generate complex absorption spectra; refer to (→Golimowski et al. 2004). **Unlike primordial brown dwarfs**: These entities of pure hydrogen have nearly ideal Planck's spectra that become the microwave background ($1460\,K / 535 = 2.73\,K$), due to a redshift of $z \sim 534$).

2.11 Hubble Radius

The Hubble constant H_0 has the unit of $km\,s^{-1}\,Mpc^{-1}$, to express the increasing recession velocity commensurate to the distance of all cosmic objects. In this work I assume $H_0=70\,km\,s^{-1}\,Mpc^{-1}$, and I convert the data of cited papers where appropriate. In the **standard model**, H_0 represents the observed value in the local universe. Therefore, the Hubble radius has increased by expansion of the space during the whole cosmic evolution.

My thesis:
Converted to SI-units (international system of units) H_0 yields $H_0=2.269\cdot10^{-18}s^{-1}$.
More useful is the reciprocal value in seconds, $t_0=4.407\cdot10^{17}s$ = $13.97\cdot10^{9}\,years$. In the **Schwarzschild universe**, it constitutes the delay time of the logarithmic redshift function. It yields a **Hubble distance** $H_D=t_0\cdot c_0$ of $H_D\equiv R_U=1.322\cdot10^{26}m$ = $13.97\,Glyr$ (giga light years = billion light years) or $4.282\,Gpc$ (giga parsec).
In this model, the Hubble distance is identical with the **Schwarzschild radius** of the spherical universe, and it is invariable over time. Hence t_0 represents *not* the age of the universe!

For illustration:
A discharging function of a capacitor on a resistor is also a falling exponential curve: $U(t)=U_0\cdot\exp(-t/\tau)$, with a time constant of $\tau=R\cdot C$. The initial energy buffered in the capacitor depletes gradually. If one lays alongside the U-t-curve at the starting point $t=0$ a tangent line, this line intersects the time line $U(t)=0$ at $t=\tau$.
Along the line of a discharging function of a capacitor, the energy of each photon on its way through the curved universe reduces by $E(t)=E_0\cdot\exp(-t/t_0)$, the universe thought to be homogeneous. This relative energy-loss $E(t)/E_0$ is identical to $1/(z+1)$ and means a redshift of the photons. For $t\sim0$ respectively $z\ll1$, the exponential function converges the tangent line described above. The analogon is the linear Hubble law $H_0D=c_0z$ at the beginning of extragalactic cosmology.

2.12 (Un)critical Density

At the **standard model**, against all explicit affirmations our universe to be 4-dimensional, one often has discussions and calculations with an implicit 3-dimensional geometry. For instance, according to this, the equations to the so-called 'critical density' of the outer space ρ_{cr} is derived from a 3-dimensional sphere; refer to (⟶de Boer 2004, page 16ff).
A deviation from this density ought to determine the destiny of the universe: It should either collapse to its centre point or expand eternally. The equation is indicated by
If one assumes the mass of the universe M_u to be calculated by means of the **Schwarzschild's**

$$\rho_{cr}=\frac{3H_0^2}{8\pi G} \quad . \qquad (1)$$

equation $M_U=\frac{R_U\cdot c_0^2}{2G}$, and the volume is computed (erroneously) three dimensional by $V_U=\frac{4}{3}\pi R_U^3$, it yields a density of $\rho_{U3}=\frac{M_U}{V_U}=\frac{R_U\cdot c_0^2}{2G}\cdot\frac{3}{4\pi R_U^3}=\frac{3c_0^2}{8\pi G R_U^2}=\frac{3H_0^2}{8\pi G}$, however where R_U is replaced by c_0/H_0. The result is identical with equation 1.

My thesis:
The **Schwarzschild universe** is a 4-dimensional sphere, so one has to calculate its volume by $V_U=2\pi^2 R_U^3$. (→Einstein 1917) mentioned this equation in his cosmological considerations.
Thus one gets $\rho_{U4}=\frac{H_0^2}{4\pi^2 G}$. In case of transformation of normal matter to a black hole, the matter spreads abrupt to a 4.71-times volume! Even the volume of the whole universe is 4.71-times bigger and its density 4.71-times less, compared to a 3-dimensional sphere. A bigger part of any 'missing' mass in the universe can be explained. This density is 'critical' by no means, because the mass is captured outwards and inwards on the 3-dimensional 'surface'. The **Schwarzschild universe** not only operates at a certain 'critical' size, but it is good-natured in a wide range. Nevertheless it is physically accurately determined by R_U (refer to table 2).

For illustration:
At a 3-dimensional sphere or the terrestrial globe, one must not confound its surface with a circular plane area of the same radius. It only yields one fourth part of the surface of the sphere.

2.13 Extragalactic Space

One can see it at the discussions of the physicists before 1930: It was clear that the really empty space is degenerated. Just the absolute empty space is a geometrically flat space. Even one atom per m³ or one atom per km³ is not empty!

My thesis:
At the first calculations of the field equations, Einstein assume an empty matter-energy tensor at infiniteness. To illustrate curved spaces at the scale of the solar system, it is negligible, whether the surrounding cosmos has a radius of curvature with a range of

$R_U = 10^{25} m, 10^{26} m$ or ∞. (→Einstein 1916) writes explicitly that the linear and orthogonal coordinate system serves as a first approximation to simplify the local field equations, and must not at all to be generalised.
In the year 1916, the extragalactic space was not established. In my view, one may not conclude once and for all that the extragalactic cosmos, we know to date, is a Newtonian or a Minkowski's space. (→Einstein 1917) wrote in his cosmological considerations that he failed to arrange the limiting conditions ad infinitum, and he plead for a closed universe with a constant density of matter. This leads in his equation 6 to a matter tensor of $T^{\mu\nu} = 0$, with the exception of $T^{44} = \rho$, the density of matter.

For illustration:
The vacuum of the extragalactic space is ideal compared to a extreme technical vacuum on earth, but not totally zero ($p \approx 10^{-11} mbar \approx 10^{11} m^{-3}$ particles). In outer space, there is on average rarely more than one hydrogen atom per cubic metre, but in a cube of $325 Parsec \approx 10^{19} m$ edge length, one can find matter of one solar mass $(M_\odot \sim 2 \cdot 10^{30} kg)$!

3 Key Figures of the Schwarzschild Universe

In table 2, one finds figures with four valid digits. It doesn't mean that the radius and all other values, derived from the radius, are known with such an accuracy.

table 2: Key figures of the Schwarzschild universe at $H_0 = 70\,km\,s^{-1}\,Mpc^{-1}$

Quantity	Equation
Radius: $13.97 \cdot 10^9\,light\ years = 1.322 \cdot 10^{26}\,m$ (≡ Hubble-Distance, chapter 3.1)	$R_U = c_0 / H_0$ *(2)*
Circumference: $87.78 \cdot 10^9\,light\ years = 8.306 \cdot 10^{26}\,m$ (chapter 3.1)	$U = 2\pi \cdot R_U$ *(3)*
Mass: $8.900 \cdot 10^{52}\,kg = 4.776 \cdot 10^{22}\,M_\odot$ (chapter 3.2)	$M_U = \frac{R_U \cdot c_0^2}{2G}$ *(4)*
Volume: $4.556 \cdot 10^{79}\,m^3$ (chapter 3.2)	$V_U = 2\pi^2 \cdot R_U^3$ *(5)*
Density: $1.954 \cdot 10^{-27}\,kg/m^3$ (chapter 3.2)	$\rho = M_U / V_U = \frac{c^2}{4\pi^2 \cdot G \cdot R_U^2}$ *(6)*
Content of energy: $7.999 \cdot 10^{69}\,J$ (chapter 3.3)	$E_U = M_U \cdot c_0^2$ *(7)*
Density of energy: $1.756 \cdot 10^{-10}\,J/m^3$ (chapter 3.3)	$\omega = E_U / V_U$ *(8)*
Redshifts: Relevant range: 0~z~534 **Distances:** Relevant range: 0~ $D_{\log}$ ~ $88\,Glyr$; equal to the circumference U of the universe. (chapter 3.4)	$z = \exp(D_{\log} / R_U) - 1$ *(9)* $D_{\log} = R_U \cdot \ln(z+1)$ *(10)*

3.1 Radius and Circumference

The today's valid **standard model of cosmology** makes no commitment our universe to be spherical, hyperbolic, or 'flat'. 'Flat' primarily means in this model that there is no geometric curvature, and in a modern interpretation that the universe is in an equilibrium state between expansion and shrinking. Often one can read the opinion that the curvature of the today's universe has become so marginal to be neglected confidently; refer for instance to (→ Schneider 2008, page 174). A flat or hyperbolic geometry also implies the universe to be open, in contrast a spherical universe is closed and finite but boundless.

My thesis:
This paper assumes that the universe is spherical and 4-dimensional, in which the whole matter forms a **Schwarzschild sphere** with the radius R_U. I remodel the equation 4,

$$\frac{R_U}{M_U} = 2G\varepsilon_0\mu_0 = 1.485 \cdot 10^{-27}\, m/kg \quad , \qquad (11)$$

established by (→ Schwarzschild 1916), to emphasize that not a *certain* radius or a *certain* mass of the universe depends on the three fundamental constants G (gravitational constant), ε_0 (electric field constant) and μ_0 (magnetic field constant), but only its ratio. Moreover one needs no additional assumptions or further natural constants to explain the dimensions of the universe. The whole universe doesn't rotate. The circumference has the value $2\pi \cdot R_U$ like at every sphere. It is time, after over 100 years of extragalactic cosmology, to determine the accurate size and shape of our cosmos.

3.2 Mass, Volume, and Density

There is no accurate statement about mass, volume and size of the **standard universe**.
But in the Schwarzschild universe, all data depends firmly on its radius. For all figures and equations at $H_0 = 70\, km\, s^{-1} Mpc^{-1}$ refer to table 2.

3.3 Energy Content and Density

In the to date's **standard model of cosmology**, the vacuum energy ϵ_Λ is derived from the quantum field theory. It has a order of $\epsilon_\Lambda \approx 10^{109}\, J\, m^{-3}$ $\left(10^{110}\, erg\, cm^{-3}\right)$; refer per example to (→ Carroll 2001, page 9).
Furthermore, there is an enormous kinetic energy, caused by Big Bang that should be nearly dissipated by space expansion and converted into potential energy nowadays.

My thesis:
One can calculate the vacuum energy in the **Schwarzschild universe** simply on the lines of Einstein's equation to the equivalence of mass and energy $E_U = M_U \cdot c_0^2 = 8.00 \cdot 10^{69}\, J$. It yields an averaged energy density over $4.556 \cdot 10^{79}\, m^3$ of $\epsilon_U = \rho_U \cdot c_0^2 = 1.756 \cdot 10^{-10}\, J\, m^{-3} \left(1.756 \cdot 10^{-9}\, erg\, cm^{-3}\right)$. This value is not changeable over cosmic times, but is affected by local mass accumulations.

To my knowledge it wasn't broached the issue that out of the hot primordial plasma there should have built **matter and antimatter** in equal parts after cooling down. As one finds hardly antimatter in the cosmos, 99.99...% of all matter and antimatter should have irradiated to pure energy. The fraction of matter to be observable today, should be a vanishing small fraction of the whole mass-energy of the universe, even when the postulated dark matter and energy is included. The asymmetry of matter and antimatter also isn't explained. Thus the total energy of the universe should be much bigger than $8.00 \cdot 10^{69}\, Joule$ mentioned above.

My thesis:
Similar to **Dirac's 'Sea of Antimatter'**, antimatter is the interior view of our ordinary matter, if one could approach the inner side of the 3-dimensional 'surface' of the 4-dimensional cosmos. There the time lapse turns back; all amassments are located on gravitational heights and hills. Particles and celestial bodies run 'uphill', due to the curvature of space and the reversed time lapse. This forces inhibit the universe and all black holes to become singularities.
Antiparticles could be forced by particle accelerators to the 'wrong' side of the cosmos, where they irradiate at once by annihilation.

3.4 Redshift in the Schwarzschild Universe

(→ Shapiro 1964) is concerned with the delay of radar echoes scraping past the sun's surface.
(→ Shapiro et al. 1968) succeed to determine this delayed echoes for the first time.
(→ Bertotti, Iess & Tortora 2003) use the radar signals of the Cassini-spacecraft, which is located between Jupiter and Saturn in the year 2002, to measure accurate signal delays. They also determine a negative **frequency shift** for the first time.
Physicists obviously don't associate this frequency shift with the redshift of single photons in curved spaces!

My thesis:
If radar signals or other photons incur a (slight) deflection due to gravitation, they suffer energy-loss and therefore a redshift, proportional to the deflection angle α near local masses, as well as in the 'empty' universe. When the light of stars passing the sun, it

deflects $1.75'' = 8.484 \cdot 10^{-6}$ and it sustains a redshift of $z = 4.848 \cdot 10^{-6}$.
For small deflection angles $\alpha \gg 1$ directly at a Schwarzschild-radius, one can also apply the linear equivalence principle $\alpha = z$: i. e. one arcsecond deflection of photons leads to a redshift of $z = 4.848 \cdot 10^{-6}$. At the Schwarzschild radius of the universe $1.75'' = 8.484 \cdot 10^{-6}$ deflection is equivalent to a distance of 67.7 klyr ($6.41 \cdot 10^{20} m$) at $H_0 = 70\, km\, s^{-1} Mpc^{-1}$.

3.5 Special Locations

In the Schwarzschild universe, there are special locations like on the three dimensional earth globe, however relative to the observer, not to the north pole. At a certain distance, where the angle of the position vector is 90°, one finds a sphere, named the '**equator of the cosmos**'. On the observer's opposite side of the cosmos there is a point to name '**opposite pole of the cosmos**'. When the light surrounds the cosmos once, it achieves the place of origin, the '**self-pole of the cosmos**'. On its way from the opposite pole to the self-pole, the light passes the '**anti-equator**' after further 22 billion years. All these special locations feature the scale of projections of celestial objects (refer to chapter 4.4). There are complementary locations near the above mentioned special location: There one observe the same angular distances D_A' like in the local universe, i.e. before the opposite pole and behind the opposite pole one observe for example $D_A' = 3.814\, Gpc$ at z=2, and $D_A' = 4.28\, Gpc$ at z=4, although the distance $D_{\log}$ increases steadily with redshift. (refer to figure 1 and the examples at chapter 5.10). At z=4, the location 'jumps' behind the equator at z=3.81.

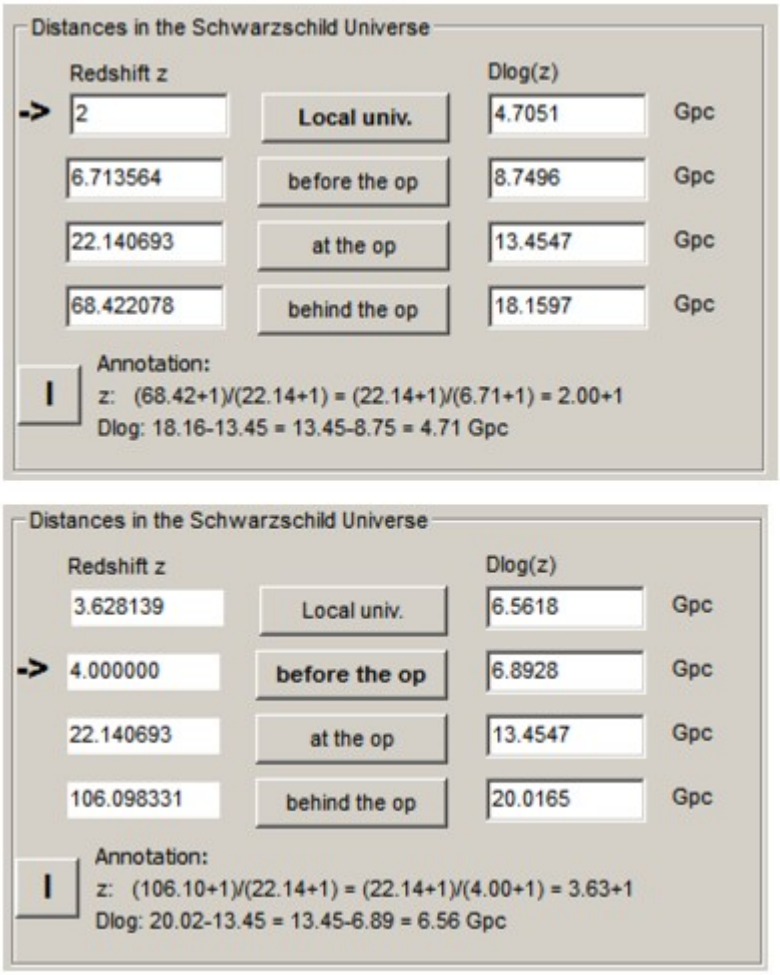

Figure 1: Complementary locations for z=2 and z=4

4 Gravitational Effects

4.1 Loss of Energy, generally considered

Einstein's paper (→ Einstein 1915) deals with the perihelion rotation of Mercury around the sun. In his paper, he remarks no relationship to gravitational waves. But corresponding to his General Theory of Relativity, every *accelerated* mass suffers an energy-loss due to gravitational waves (first mentioned at → Einstein 1916). There he distinguishes longitudinal waves and transverse waves that irradiate no energy, but only warp the coordinate system. In contrast, three other types of gravitational waves transport energy. He also notices that electrons at there movement around atom cores should actually irradiate electro-magnetic waves and gravitational waves, but they obviously don't. So he disbelieves his own considerations. In the year 1916, quantum theory isn't well established yet.
As we know nowadays, electrons arrange in quasi-stationary clouds around their atom cores. There is no movement. (→ Einstein 1918) re-handles gravitational waves. He suspects that 'thermal agitation', i.e. submicroscopic thermal fluctuations of atoms and molecules cause also gravitational energy-losses, but he is in doubt. Even more, he doesn't mention that photons that are hindered to propagate rectilinear loose energy by gravitational waves. This implies that photons would be redshifted.
Anyway (→ Zwicky 1929) discusses elaborately different mechanism of cosmic redshift without expansion of space or Doppler effect that could lead to redshift of single photons. Thereby he makes rough calculations and mentions gravitational waves as potential causation. (→ Eddington 1930) designates speculative redshift without expansion as 'gravitational friction'.

My thesis:
In physics, **gravitational waves** were strongly underestimated nowadays. They are omnipresent, they appear in all amplitudes and wave length and they **are not quantised**. At thermal movements of elementary particles, energy-losses by electro-magnetic waves are many orders bigger than losses by gravitational waves. The exception are ultra-thin and ultra-hot plasmas in interstellar media: Gravitational waves boost their temperature to many million degree centigrade, before UV and gamma rays can dissipate the energy. If it won't be successful to to determine a rest mass to **neutrinos**, it could be considered to assign that subatomic effects to gravitational waves that are referred to neutrinos to date. One should also refer gravitational waves to the radioactive β-decay.
Even photons lose energy by gravitational waves, when they cannot propagate straightforward. In a spherical 'empty' space, nothing and nobody can fly rectilinear. And because photons keep their velocity, energy-loss manifests in redshift, i.e. their wavelength increases. The cosmological redshift without Doppler effect or expansion of space was disparaged as '**tired light**'. Photons that passes a massive local object passes an

additional space curvature. That causes not only a non-reversible change of the direction, but also an additional non-reversible energy-loss by gravitational waves.

4.2 Primordial Texturing due to Energy-Losses

At the beginning of the **Schwarzschild universe**, there was no friction. Friction means interdependence of agitated matter that emits light quanta to the surrounding space and if applicable, to uninvolved matter. Quantum fluctuations that chance minimally the positions of all hydrogen atoms, compensate itself statistically. If one will not postulate '**primordial fluctuations**', one has to assume that a fractional part of the displacements are not equalised, because meanwhile the hydrogen atoms have delivered gravitational energy. At the beginning era, gravitational losses took the function of electro-magnetic friction. All tiny movements of particles are partly irreversible. This displacements lead over trillions of years to the large-scale structures that we denominate 'voids' and 'filaments'. Computer-simulations of the expansive standard model are calculated since decades (refer to → Springel et al. 2005). These simulations often are distinguished by calculating firstly the evolution of the pure non-baryonic dark matter, and adding a small percentage of common baryonic matter afterwards. These simulations are also useful for the **Schwarzschild universe** and could be repeated with small modifications and with modern computing power.

4.3 Proceeding of Perihelion of Mercury and Twin-Pulsars

The double-pulsar-system PSR B1913+16 shows an apsidal precession of $4.2\,°/\mathit{year}$ and is observed for decades. This strong apsidal precession can not be explained by common (tidal-) friction. It is presumed to be an indirect evidence of energy-losses by gravitational waves (e.g. refer to →Weisberg et al. 2010). The indirect evidence of energy-losses by gravitational waves of other, even much more energy-rich incidences has been succeeded by LIGO in many cases. The LIGO's signals are conceded to be signatures of merging black holes (e.g. refer to →LIGO 2019).
A much more subtle effect that obviously is not recognised to be an effect of gravitational waves, is the additional perihelion precession of the Mercury's orbit around the sun. The nearest point of the elliptical orbit precedes 0.43" per year in the direction of revolution. (→ Einstein 1915) calculated this in his paper of General Relativity. He writes even explicitly that perfect circular orbits have no perihelion precessions, although his equation (in my paper equation 12) leads to a precession angle unequal zero. The double-pulsar-system PSR B1913+16 wasn't known in 1915.

My thesis:
Einstein calculated the perihelion precession of planets and gravitational waves in separated papers. For the perihelion precession, he calculated first and second approximations. Obviously escaped him the fact that there is a causal relationship between both effects: Mercury continuously looses kinetic energy on its orbit around the

sun due to gravitational waves. The orbit shrinks and Mercury accelerates! Gravitational energy-loss is the primary effect, it causes secondary the 'perihelion precession', even at circular orbits. The eccentricity of the orbit leads to disproportionately increasing energy-losses at equal frame conditions (refer to equation 18).

I will deduce the equivalence of the equation of the apsidal precession of binary neutron stars or black holes, and the equation to the perihelion precession of Mercury (and other planets): At (→Einstein 1915), one finds the equation for the perihelion precession ε *for one orbit* of Mercury:

$$\varepsilon = \frac{24\pi^3 a^2}{T^2 c_0^2 (1-e^2)} \quad . \tag{12}$$

a is the semi-major axis of the planet's orbit, T the period of the orbit and e the numeric eccentricity. (→Weisberg et al. 2010) specify the apsidal precession *per second* $\langle \dot{\omega} \rangle$ of two stars with:

$$\langle \dot{\omega} \rangle = \frac{3G^{2/3}}{c_0^2} \left(\frac{P_b}{2\pi} \right)^{-5/3} (1-e^2)^{-1} (m_1+m_2)^{2/3} \quad , \tag{13}$$

where the orbital period is tagged with P_b. One can divide equation (12) by T:

$$\langle \dot{\omega} \rangle = \frac{\varepsilon}{T} = \frac{24\pi^3 a^2}{T^3 c_0^2 (1-e^2)} \quad . \tag{14}$$

Now Kepler's equation $T^2 \propto a^3$ is quoted:

$$T^2 = \frac{4\pi^2 a^3}{G(m_1+m_2)} \quad , \tag{15}$$

and transformed to a^2:

$$a^2 = \left(\frac{T^2 G(m_1+m_2)}{4\pi^2} \right)^{2/3} = \frac{T^{4/3} G^{2/3} (m_1+m_2)^{2/3}}{4^{2/3} \pi^{4/3}} \quad . \tag{16}$$

Inserting a^2 to equation (14), it is equivalent to equation (13) and gives

$$\langle \dot{\omega} \rangle = \frac{24\pi^3 T^{4/3} G^{2/3} (m_1+m_2)^{2/3}}{T^3 c_0^2 (1-e^2) 4^{2/3} \pi^{4/3}} \quad , \tag{17}$$

because $\frac{T^{4/3}}{T^3}=T^{(4-9)/3}=T^{-5/3}=P_b^{-5/3}$, $\frac{\pi^3}{\pi^{4/3}}=\pi^{(9-4)/3}=\pi^{5/3}=\frac{1}{\pi^{-5/3}}$, and $\frac{24}{4^{2/3}}=3\cdot 2^3\cdot 4^{-2/3}=3\cdot 2^3\cdot\left(2^2\right)^{-2/3}=3\cdot 2^{(9-4)/3}=3\cdot 2^{5/3}=\frac{3}{2^{-5/3}}$.

These coefficients belong to $\left(\frac{P_b}{2\pi}\right)^{-5/3}$ and $3G^{2/3}$. The term $\frac{(m_1+m_2)^{2/3}}{(1-e^2)}$ leaves unchanged.

(→Peters & Mathews 1963, equation 16) designate energy-losses $\langle P\rangle$ by gravitational waves as a reason for the apsidal precession. The orbital equation is derived by Fourier analysis.

$$\langle P\rangle=\frac{32G^4}{5c^5a^5}\left(1+\frac{73}{24}e^2+\frac{37}{96}e^4\right)\left(1-e^2\right)^{-7/2}m_1^2m_2^2(m_1+m_2)\,. \qquad (18)$$

Deviations from a circular orbit mean harmonic waves of the orbital movement and account disproportionately for the power-losses of the systems:
(→Weisberg et al. 2010) pick up this equation and show that these energy-losses are steadily increasing with time ($\dot{P}_b^{GR}$ is the rate of change of the energy radiation):

$$\dot{P}_b^{GR}=\frac{192\pi G^{5/3}}{5c^5}\left(\frac{P_b}{2\pi}\right)^{-5/3}\left(1+\frac{73}{24}e^2+\frac{37}{96}e^4\right)\left(1-e^2\right)^{-7/2}m_1m_2(m_1+m_2)^{-1/3}\,. \qquad (19)$$

Over years, the orbital period of the double-pulsar system shortens faster and faster in form of a parabolic function; refer to (→Weisberg et al. 2010, figure 1). Weisberg et al. calculate the energy-loss to nearly $\langle P\rangle=10^{25}W$ for PSR1913+16, corresponding equation 18.
My calculation for the system sun-Mercury yields only 90W power-losses by gravitational waves, at my opinion much to low.

4.4 The 'Cosmolensing Effect'

At the **standard model**, the cosmos often is discussed like a 3-dimensional euclidean space with an additional time axis. In this space, light rays from a point source diverge quadratically with the distance to the light source. After radiation, the photons take part in the expansion of space. This is not the case at a space, which is bent to a 4-dimensional hyper-sphere.

My thesis:
The **Schwarzschild universe** is a 4-dimensional hyper-sphere of invariant size.
Individual light rays don't propagate on perfect straight lines, but on circular paths. Their curvature radius have the origin at the central point of the hyper-sphere (great circles).
The divergence of light rays from a point source is smaller than in an euclidean space. In the Schwarzschild universe, the angular sum of triangles is bigger than 180 degrees. At a certain distance from the observer, there is the **equator of the cosmos**, it is a surface area of a sphere! At that place, the divergence becomes zero and inverts to a convergence.

The geometry of the cosmos operates like a **converging lens** with a magnification factor depending on the distance. I will name this effect '**cosmolensing effect**'.

The transformation factor for distance values due to cosmolensing yields <1, i.e.

$$\frac{[D_{lum}'']}{[D_{lum}']} = \sin(\ln(z+1)) \cdot (\ln(z+1))^{-1} \cdot \qquad (20)$$

D_{lum}' is the luminosity distance due to redshift in the **standard model** (refer to equation 26), and D_{lum}'' the complete luminosity distance in the **Schwarzschild universe**. At the observer's opposite side of the cosmos, there is a focal point, where all light rays, sent from the observer's place, bundle again and vice versa, the '**opposite pole of the cosmos**'. There occur much magnified projections of '**ghost-galaxies**'. The observed images are **infrared galaxies**, because the redshift to the opposite pole is about 22 (refer to chapter 6.2.1).
On its further propagation, the light returns back to its origin point (**self-pole**), bundled again to a focal point. The redshift of this projection has the value of about 534.
There, the origin matter of our own galaxy is located, as it was distributed 88 billion years ago, projected as **microwave background** on the whole sky (refer to chapter 2.1 and 6.1.1).
(→Eddington 1930) regarded ghost-galaxies as a refutation to Einstein's spheric universe, and he considered a high redshift due to expansion of space. Thereby ghost-galaxies should elude their visibility to infrared. At that time, he could not know that galaxies emit a considerable amount of ultraviolet light that is redshifted to the optical range.

For illustration:
One can visualise the lensing-effect on an (earth-) globe, whose surface serves as a 2-dimensional model for the 3-dimensional cosmos: The north-pole should constitute the light source and the meridians the propagating light rays. The distance of the meridians along a certain circle of latitude is the measure for the 'light dilution', which increases **less than linear** (in the 3-dimensional space '**less than quadratic**') with the distance to the north-pole. The dilution achieves a maximum at the equator. At the south-pole all meridians (i.e. the light rays) focus again. That is quite the contrary to a point-source on an plane sheet, where the circumference of the concentric circles increases infinitely and linear to the radius. The light, respectively the traveller on the globe, can definitely pass by the south-pole (i.e. the **opposite-pole of the cosmol**), travelling back to the north-pole, the '**self-pole of the cosmol**' of the Schwarzschild universe. There is the second focus.

4.5 Translucent Projections

Figure 2: Arp 220, combined images of HST and JWST

One can see it at figure 2: The galaxy ARP 220, recognised as an infrared galaxy, should cover all the orange stains (i.e. redshifted galaxies at the background), if it actually stood at the foreground. Instead of this, the redshifted galaxies are completely visible. The reason is, because ARP 220 is much farther than the reddish 'background-galaxies' in the Schwarzschild universe. ARP 220 has actually a much higher redshift. So the **cosmolensing effect** affects much more ARP 220, supposing ARP 220 is a z-21.9-galaxy and the reddish galaxies are z~3.6-galaxies. Thus ARP 220 has a 100-times bigger linear magnification compared to the magnification of the other galaxies, although the former is twice far away as the latter ($D_{\log}=43.7\,Glyr$ instead of $21.3\,Glyr$).

There is also an magnification at the **standard model** by space expansion: The farther galaxy mentioned above is magnified only 3-times compared to the nearer galaxies.

4.6 Circumvention of Optical Barriers

Contrariwise, the infrared galaxy is *not* covered partly by the true foreground-galaxies. The light of the infrared galaxy (in the vicinity of the opposite-pole) completely fan out and crosses nearly all locations of the universe. Light being absorbed by a barrier at a certain part of the cosmos (by an other galaxy or a hydrogen cloud), arrives most probably the observer on many other ways.

My thesis:
The infrared spectrum of the IR-galaxy blend with the foreground galaxies, especially the e**mission lines** erroneously are ascribed to the IR-galaxy.
Absorption lines of the **Lyα-forest** are circumvented and could be affectless.

For illustration:
If one covers partly the front lens of a telescope with small stains, they don't appear in the visual field of the observer. In fact the projection is dimmer than without stains.

4.7 Multiple Pictures

Eddington predicted common **gravitational lenses** (→Eddington 1920). There are manifold problems by determining the properties of gravitational multiplex projections and Einstein's arcs, which seem to confirm the standard model: One has huge differences of the indication of distances and the mass of the foreground galaxies respectively the galaxy clusters between standard model and Schwarzschild universe.
A recent study is concerned with the determination of the Hubble Constant by modelling the multiple gravitational lenses B1618+656 and RXJ1131-1231 (→Jee et al. 2019). They ascertain a value of $H_0 = 82.4\,(+8.4 - 8.3)\,km\,s^{-1}\,Mpc^{-1}$ and comment that it doesn't fit to the value of $H_0 = 67.3\,km\,s^{-1}\,Mpc^{-1}$, calculated by the (→Planck Collaboration 2014/16) on the basis of the microwave background. The latter quantity only yields 82% of the former. To indicate the age of the universe with two positions after decimal point is completely exaggerated!

My thesis:
1. At the standard model, the mass of a bending foreground galaxy (or galaxy cluster) is determined by the velocity dispersion of its components on the basis of the width of the spectral lines. Thereby, the radiation of gravitational waves is not considered. Instead of this, a huge amount of dark matter is supposed like Zwicky 1937 did. The bending impact to the light rays enlarges with increasing mass: The calculated distances of the background objects get smaller, and the Hubble constant bigger. I predict that this accounts the biggest error at H_0 at the standard model.

2. On the other hand, there is a difference between the smaller light travel time and the comoving distance D_{com} at the standard model. In contrast to that, the light travel time and the logarithmic distance $D_{\log}$ are equal at the Schwarzschild universe, but somewhat bigger than D_{com}. As a result, the Hubble constant is smaller than calculated at the standard model.
3. Furthermore, the transverse angular distances of the multiple projections were overestimated, because the presumed angular expansion at the standard model is much more bigger than the Cosmolensing effect of the Schwarzschild universe. Not before z=19.4, the Cosmolensing effect overruns the assumed space expansion. So less bending mass is necessary.
Should ever be possible to measure deviations of redshift at the order of $\Delta z \sim 10^{-6}$, the differences of asymmetric multiplex projections of quasars could be analysed systematically.

5 Conversion from Standard Model to the Schwarzschild Universe

5.1 Luminance of Celestial Bodies

Before Galilio Gallilei, astronomers depend solely on visual observations of the starry sky. According to the conception of the middle age, fixed stars were attached to a sphere of unknown distance. The stars were divided into six size categories (magnitudes, abbr. mag). The brightest stars were assigned to the 1. magnitude, stars even to be visible with the naked eye were assigned to the 6. magnitude (without decimal places).
The break-even value extended on visual observations to 13mag by means of increasing telescopes (at 200mm aperture at best seeing), by introduction of photography to further 2.5mag (at equal optical systems).
The 10m Keck Telescope on the 4200m high Mauna Kea achieves, due to thin and dry air and adaptive optic, a break-even value of 26mag, and the Hubble space telescope (HST) 31mag. Thereby, the angular resolution of the observation chain has to keep up, to determine the distance ladder by parallax measurement. At best the resolution of the human eye comprises 2' to 1' (arc minutes). A 200 mm amateur telescope achieves about 0.6'' (arc seconds), the HST about 0.05'' .The relative luminosity of two stars is defined according to the logarithmic sensitivity of the eye

$$m_1 - m_2 = -2.5 \log\left(\frac{S_1}{S_2}\right) , \qquad (21)$$

where S_1 and S_2 are the observed radiant fluxes and m_1 and m_2 the apparent magnitudes.

The reference magnitude of Wega (αLyr) was determined to $-0.01\,mag$ by photographs near the polar star (North polar sequence) and later by modern proceedings.

5.2 Distances in Cosmology

The apparent luminosity at the observer states nothing about the absolute luminosity of a celestial body.

$$S=\frac{L}{4\pi D^2} \qquad (22)$$

The observed radiant flux S depends on the absolute radiant power L and the distance D, regardless of further attenuating factors by the interstellar space, the earth's atmosphere and the observing technology. 1838 Friedrich Wilhelm Bessel was the first to use the parallax measurement of stars. Over the decades, the absolute distances of many important stars could be investigated. For instance, Vega has a distance of 25 light years = 7.68 pc (parsec) = $2.37\cdot10^{17}\,m$. Thereupon the absolute magnitude M was determined to a reference distance of 10pc:

$$M=m-5\log\left(\frac{D}{10\,pc}\right) \qquad . \qquad (23)$$

Thus the sun, due to the vicinity to the earth ($149.6\cdot10^{9}\,m$ = one astronomical unit = 1 AU = $4.848\cdot10^{-6}\,pc$), has only an apparent magnitude of $m=4.74$ at 10 pc. This is by definition the absolute magnitude $M_{\odot}$ of the sun, a rather pale star. Owing to the vicinity it appears with a magnitude of about $m=-27$. The luminosity power of the sun $(L_{\odot})$ = $3.828\cdot10^{26}\,W$ often serves as a reference quantity for the luminosity of other celestial bodies.
With the parallax method, one can reach distances of several 100 pc. For the leap to the extragalactic cosmos, the period-luminosity relation of bright variable stars is needed. Subsequent to this, one needs the relation between redshift and distance. Finally it is a question of some giga parsecs. Edwin Hubble was concerned with these questions from the 1920s.

5.3 Distances in Cosmology

(→Hubble & Humason 1931) assumed a linear ratio between distance and redshift. At today's sight it is quite understandable. At that time, the observed redshifts reached up to $z\sim0.01$ and the comoving distance D_{com} is just $0.25\,\%$ smaller than the linear distance (about 42.7 Mpc to 42.8 Mpc at $H_0=70\,km\,s^{-1}\,Mpc^{-1}$). In contrast, Hubble **overestimated** the expansion rate initially $v_E\sim500\,km\,s^{-1}\,Mpc^{-1}$, thus an **underestimation** of the distances at least of 7.
In the **standard model**, it is accepted that the spaces expanded more and more over trillions of years. Light ray irradiated by celestial bodies, take part in the space expansion and spread to an increasing space volume. Thereby galaxies are not subdued to this expansion, called

'Hubble-Flow'. Farther objects have higher escape velocity than nearer. Similar to the Doppler effect, one can see a redshift $z=\Delta\lambda/\lambda_0$; the observed wavelength of the light is extended, compared to the rest wavelength. Thus a light source determining a redshift z , has an additional attenuation to the conventional distance luminosity law $L\propto 1/D^2$ of $(z+1)^{-2}$, because in addition to the energy-loss of every single photon, one gets a smaller photon rate of $(z+1)^{-1}$. So there are different distance measures, i.e. the light travel distance D_P ('proper distance'), the comoving distance D_{com} (at line of sight), the transverse moving distance D_M , the luminosity distance D_{lum} , and the angular (diameter) distance D_A . It depends on the effects of the expanding space to be considered, at the conversion of observational data to the true features of the light source.

Further one has the linear Hubble law $D_H \equiv \frac{z\cdot c_0}{H_0}$ for small distances $(z \ll 1)$.

Hogg 1999 indicates at his 'cheat sheet' for cosmological distances that different authors name individual terms variably or use them in a different way. Corresponding to Hogg, all figures are related to the critical density $\rho_{cr}=\Omega_M+\Omega_\Lambda+\Omega_k=1$, where Ω_M is the ratio of baryonic matter, Ω_Λ the ratio of dark energy and $\Omega_k=0$ ratio of the curvature of space. The curvature zero means that the universe is flat and it neither expands nor shrinks. $\Omega_k=0$ also means that one need not make a difference between D_M and D_P ; refer to (→Hogg 1999, equation 16). Small sections of δD_{com} are defined by $E(z)\equiv\sqrt{\Omega_M(1+z)^3+\Omega_k(1+z)^2+\Omega_\Lambda}$ and have to be integrated by $D_{com}=D_H\int_0^z \frac{dz'}{E(z')}$. At D_{com} , the measuring rod of the observer increases along the line to the space expansion and therefore it is the fundamental distance measure at the **standard model**. One can derive the other distances directly from D_{com} : The angular distance $D_A=\frac{D_{com}}{z+1}$ is valid for objects of similar distances, observed with an angle at the sky. The luminosity distance $D_{lum}=D_{com}\cdot(z+1)$ is valid for objects, which distances can be determined by the ratio of apparent to absolute luminosity.

Furthermore, there is a **cosmological time dilation** at the standard model. It effects the deceleration $(z+1)^{-1}$ of the observed lapse of time, compared to the local lapse of time.

My thesis:

In the **Schwarzschild universe,** there was and there is no space expansion and therefore no difference between comoving and proper distance. Galaxies are at rest except for their peculiar velocities of some $100\,km/s$; this is even valid for galaxies being far away from the observer (high-z galaxies).

Instead of this, there is a simple redshift-distance law: $z=\exp(D_{\log}/R_U)-1$ (refer to equation 9) and the inverse function: $D_{\log}=R_U\cdot\ln(z+1)$ (refer to equation 10).

$D_{\log}$ may be predicated '**logarithmic distance**' or '**logical distance**'.

5.4 Comoving Distance

D_{com} and $D_{\log}$ are the corresponding distances at the **standard model** and the **Schwarzschild model**. In the range about of 0 < z < 7, the comoving distance D_{com} is bigger than the new

$$\mu = m - M = 5\log\left(\frac{D_L}{10\,pc}\right) \qquad (24)$$

logarithmic distance $D_{\log}$ (refer to figure 3 and 4). At higher redshifts, $D_{\log}$ outperforms D_{com}, because D_{com} approaches asymptotically the age of the standard universe of about $14.0\,Gpc / 45.6\,Glyr$ (refer to figure 5). The proper intersection of the two plots has to be determined be accurate observations.

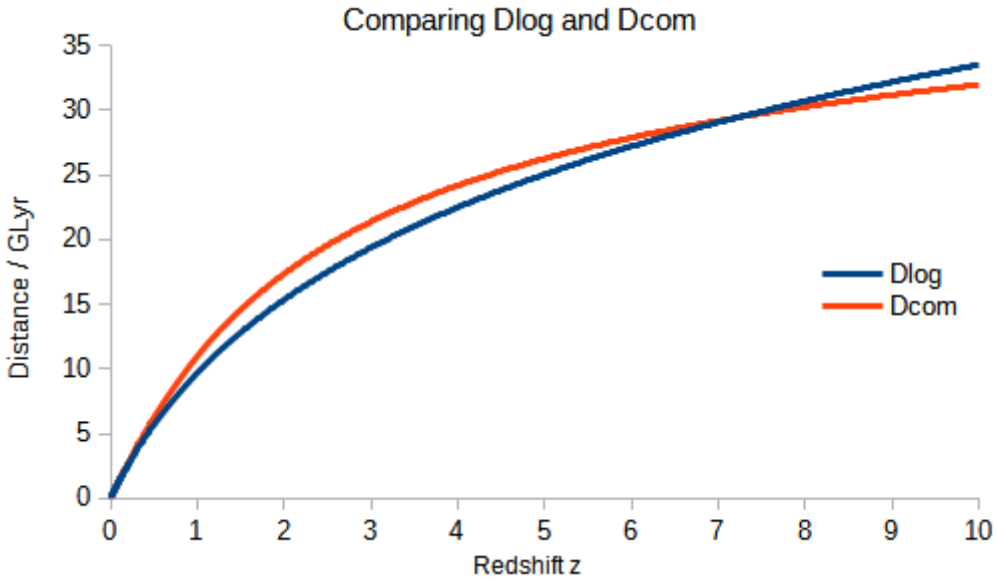

Figure 3: Redshift range 0<z<10

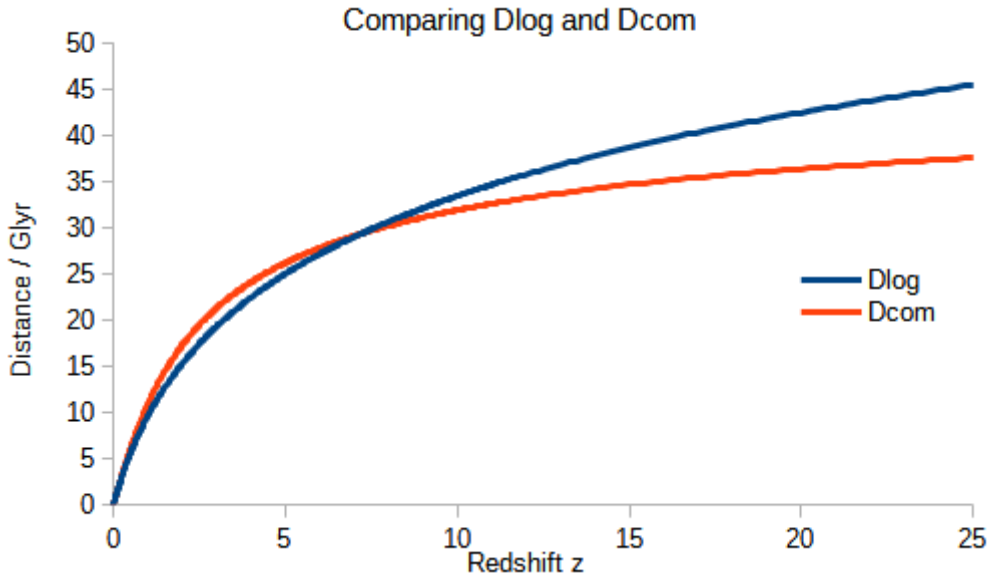

Figure 4: Redshift range 0<z<25

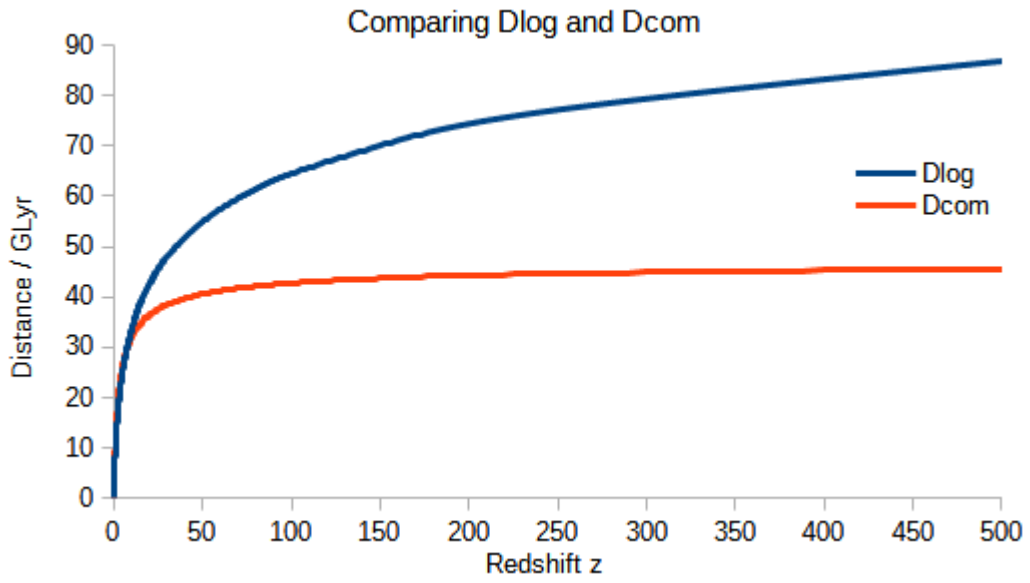

Figure 5: Redshift range 0<z<500

5.5 Luminosity Distance

At cosmological distances, one has to incorporate the impact of the redshift that diminishes the apparent luminosity and enhances the indication of distances. At the standard model, one has to insert the luminosity distance D_{lum} instead of D into the equations 22 and 23:

$$D_{lum} = D_{com} \cdot (z+1) \quad . \tag{25}$$

Owing to the lack of space expansion, there is no dilution of the photon rate in the **Schwarzschild universe**. However, the attenuation of the photons' energy persists. Under inclusion of the new logarithmic distance $D_{\log} = R_U \cdot \ln(z+1)$ (like equation 10), the luminosity distance is defined to:

$$D_{lum}' = D_{\log} \cdot (z+1)^{1/2} \quad . \tag{26}$$

Rated by the **standard model ,** one gets systematically a too high luminosity distance and a too high absolute luminosity of celestial bodies. This equation is to be applied for the luminosity distance of objects with a transient brightness curve like supernovae.

The **Cosmolensing effect** produces projections with higher angular extension without dilution of the surface brightness, compared to the euclidean space. The second step is to calculate the magnification of the images. Considering the impact of the redshift in equation 26, the luminosity distance is:

$$D_{lum}'' = R_U \cdot (z+1)^{1/2} \cdot \sin(\ln(z+1)) \quad . \qquad (27)$$

Beyond distances of about 7 Gpc ($z \approx 4$ or $\ln(z+1) \approx \pi/2$, e.g. beyond the equator), the light rays even converge. It mocks too low distances and too high absolute luminosities.

5.6 Angular Distance

The equation of the angular distance at the **standard model**:

$$D_A = \frac{D_{com}}{z+1} \quad . \qquad (28)$$

Due to the expansion of space, the transversal distance D_A grows slower than D_{com} . D_A has the peculiarity to shrink again at distances $z > 1.6$.
In contrast, the equation of the angular distance at the **Schwarzschild universe**:

$$D_A' = D_{\log} \cdot \sin(\ln(z+1)) \quad . \qquad (29)$$

It isn't enough to recalculate the lack of space expansion but one must consider the neglected cosmolensing effect (chapter 4.4).
Furthermore D_A' even shrinks beyond distances of about 7 Gpc. For the recalculation of D_A to D_A' , one has to execute three operations (refer to table 3, 4, and 5).

5.7 Surface Brightness of Celestial Objects

If one can determine the surface brightness B of a (not 'punctual') celestial body, one has to assume a dilution of the surface brightness B commensurate to redshift of $(z+1)^{-4}$ at the **standard model**. At the standard model, the apparent plane of projection increases by space expansion proportional $(z+1)^2$. Thus it is ascribed an additional dilution of $(z+1)^{-2}$ to the the surface brightness, together with the redshift and the time dilation, it sums up to $(z+1)^{-4}$ corresponding to (→Tolman 1930).

My thesis:
In the **Schwarzschild universe**, there is no expansion of the plane of projection. The surface brightness decreases proportional to the redshift of $(z+1)^{-1}$. Though the cosmolensing effect magnifies the apparent plane of projection, it has no additional effect to the surface brightness.

5.8 Transformation Software

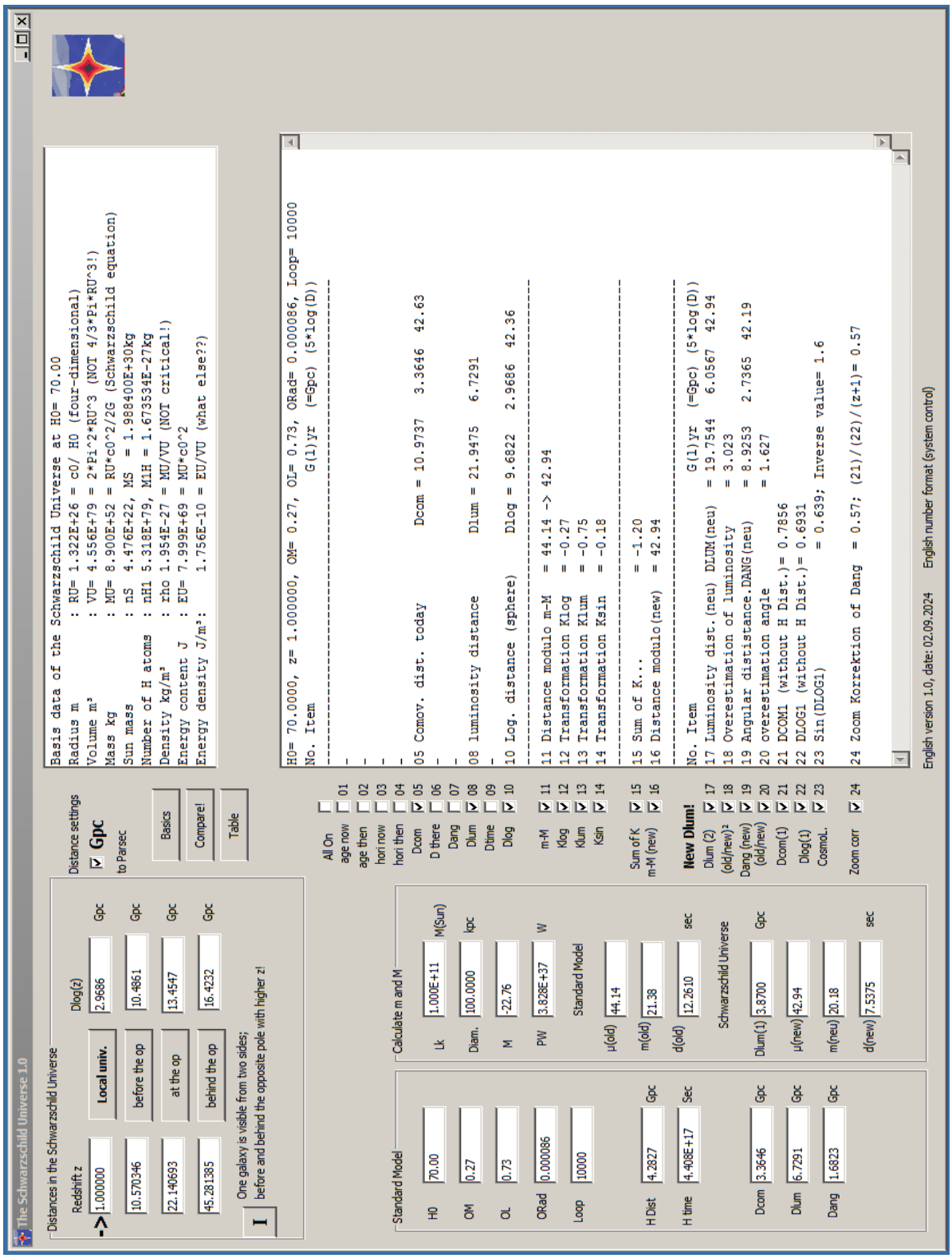

figure 6: Transformation software

The program shown in fig. 6, supports the conversion from the **standard universe** to the **Schwarzschild universe** and vice versa. In most fields, one can not only read the figures, but one can directly overwrite them. The prompt reaction is the recalculation of all fields and tables. The box [Distances in the Schwarzschild Universe] is adjusted to the special locations in relation to the observer '**ahead to the opposite pole**' and '**behind the opposite pole**' (refer to chapter 3.2, 'special locations').
The algorithm for the standard universe is based on a C-source code of (⟶Powell 2000) that calculates the particular distances D_{com}, D_{lum} and D_A and time intervals out of a given redshift. My Schwarzschild program is written in the programming language Lazarus.
In this program, one can also calculate backwards by iterations of iterations, the distances of the standard model to the distances of the Schwarzschild model, furthermore the redshifts, the distance moduli, the transformation numbers and the corresponding special locations.

5.9 Transformation Numbers

For calculation of the numbers $D_{\log}$, D_{lum}', D_{lum}'', D_A' and B' in the **Schwarzschild universe**, respectively for the conversion from the published corresponding numbers of the **standard model**, D_{com}, D_{lum}, D_A, and B, I will introduce hereinafter transformation numbers and their application.

table 3: Transformation numbers for distances and their logarithms

Step	Conversion	Coefficient for distances	Summand for $\mu = m - M$
1.	$D_{com} \Rightarrow D_{\log}$	$f_{\log} = \frac{D_{\log}}{D_{com}}$	$k_{\log} = 5 \log_{10}\left(\frac{D_{\log}}{D_{com}}\right)$
2.	$D_{\log} \Rightarrow D_{lum}'$	$f_{lum} = \sqrt{z+1}$	$k_{lum} = 2.5 \log_{10}(z+1)$
3.	$D_{lum}' \Rightarrow D_{lum}''$ resp. $D_{\log} \Rightarrow D_A'$	$f_{\sin} = \frac{\sin(\ln(z+1))}{\ln(z+1)}$	$k_{\sin} = 5 \log_{10}\left(\frac{\sin(\ln(z+1))}{\ln(z+1)}\right)$
4.	Surface brightness B	$f_B = (z+1)^{1.5}$	$k_B = 7.5 \log_{10}(z+1)$

5.10 Examples

The examples are shown with the indirection over the logarithms. As always is $H_0=70\,km\,s^{-1}\,Mpc^{-1}$, $\Omega_M=0.27$, and $\Omega_\Lambda=0.73$. The figures are extracted from the conversion program described in chapter 5.8, under the reservation of rounding errors. D_{lum}' is relevant for long-distant supernovae; their light curves are planed and widened increasingly with increasing redshift. On transient signals, the cosmolensing effect and therefore $k_{\sin}$ affects rather to the width and not so much to the maximum brightness (refer to chapter 6.4).

To transform a given absolute magnitude $M(old)$ in the standard universe of constant shining celestial objects, one has to apply

$$M''=M-k_{\text{sum}} \quad . \tag{30}$$

To get the distances D out of the distance moduli μ, one has to apply

$$D/10\,pc=10^{(\mu/5)} \quad . \tag{31}$$

table 4: Conversion of D_{lum} to D_{lum}'' for z = 2 (luminosity distance old → new)
($D_{lum}=15.96\,Gpc$ at z = 2 belongs to $D_{com}=5.32\,Gpc$ at the standard model)

Step	μ respectively k	Subtotal	Distance in Gpc
D_{lum}	$\mu_{lum}=46.02$	46.02	$D_{lum}=15.96$
1	$k_{\log}=-0.27$	45.75	(not relevant)
2	$k_{lum}=-1.19$	44.56	$D_{lum}'=8.15$
3	$k_{\sin}=-0.46$	44.10	$D_{lum}''=6.61$
	$k_{\text{sum}}=-1.92$		
Conversion of D_A to D_A' for z = 2 (angular distance old → new)			
D_A	$\mu_A=41.24$	41.24	$D_A=1.77$
1a	$2\cdot k_{lum}=+2.39$	43.63	$D_{com}=5.32$
2a	$k_{\log}=-0.27$	43.36	$D_{\log}=4.71$
3a	$k_{\sin}=-0.46$	42.90	$D_A'=3.81$
	$k_{\text{sum}}=+1.66$		

table 5: Conversion of D_{lum} to D_{lum}'' for z = 4 (luminosity distance old → new)
($D_{lum}=37.05\,Gpc$ at z = 4 belongs to $D_{com}=7.41\,Gpc$ at the standard model)

Step	μ respectively k	Subtotal	Distance in Gpc
D_{lum}	$\mu_{lum}=47.84$	47.84	$D_{lum}=37.05$
1	$k_{\log}=-0.16$	47.68	(not relevant)
2	$k_{lum}=-1.75$	45.93	$D_{lum}'=15.41$
3	$k_{\sin}=-1.03$	44.90	$D_{lum}''=9.57$
	$k_{sum}=-2.94$		
Conversion of D_A to D_A' for z = 4 (angular distance old → new)			
D_A	$\mu_A=40.85$	40.85	$D_A=1.48$
1a	$2\cdot k_{lum}=+3.49$	44.34	$D_{com}=7.41$
2a	$k_{\log}=-0.16$	44.18	$D_{\log}=6.89$
3a	$k_{\sin}=-1.03$	43.15	$D_A'=4.28$
	$k_{sum}=+2.30$		

6 Revision of Results

In relevant publications of extra galactic light sources, it is unusual to quote directly the observation data, but to transform them implicit to the absolute figures pre-specified by the **standard model**. By means of the **Schwarzschild model**, presented in this paper, the results of some research studies will be transformed. For this purpose the transformation numbers, introduced in chapter 5.9, are applied and set in contrast to the primary results. I will show that the application of Einstein's physics, using the example of the **Schwarzschild model**, delivers at least also plausible results like the **standard model of cosmology**, without using a lot of additional parameters and without features of direct evidence (refer to chapter 7).

6.1 Structure and Evolution of the Cosmos

On the surface of the of the **Schwarzschild universe**, there are all the possibilities of development, we can observe at the common **standard model**. However, the entire development takes many dimensions longer than 13.8 billion years. According to the hypothesis of Einstein, every local accumulation of matter bends the space to a potential funnel. In relation to the spheric model, its surface becomes unimposing concave dents and calderas at places, deviating from the ideal and homogen distribution of matter. Thus our sun is located in a potential funnel, which is 'three kilometres' deep corresponding to its Schwarzschild radius. A whole galaxy of $10^{11}(M_{\odot})$ shapes a potential funnel of about 0.03 light years ($d \sim 3 \cdot 10^{14} m$), compared to the radius of the cosmos $R_U \sim 1.3 \cdot 10^{26} m$ a very small figure. Even black holes don't sink deeper than their own Schwarzschild radius into the 3-dimensional surface; they fall noway to the centre point of the Schwarzschild universe and they are to this effect *no singularity*. They form to a certain extend a closed micro-universe.
The dispute, the universe to be homogen and isotropic in all directions at great scales, unravels in the Schwarzschild universe: The primordial perfect spheric symmetrical universe gets more and more inhomogeneous by perseverate evolution: At the beginning, there are solely hydrogen atoms with a density of about one atom per m³, without appreciable kinetic energy, and in uniform distribution. Photons exist not at all, because they have to be generated in aggregations of matter, the later 'celestial bodies'. These ideal pressureless matter is not inhibited to concentrate to noteworthy agglomerations by time restriction or by a primordial heatwave. On these grounds, the manifold observed **Voids and Filaments** could arise over trillion of years. According to open star cluster that often don't stand out against their surrounding, I will name the very first concentrations of gas '**open gas cluster**' or 'whiffs'.
Long before nuclear fusion of hydrogen to helium arises, there are jupiter-like gas-'planets' to emit long-wave radiation. They can agglomerate to T-dwarfs by accretion or merging, to start nuclear fusion at a surface temperature of about 1000K. In that era, they were the tip of evolution. The agglutination of matter at all ranges, one can observe nowadays, leads to the end that the bigger part of matter and photons will vanish in black holes, which will merge to one big black hole, a new universe.

My thesis:
The term' static universe' for an universe, which solely has a constant mass-energy content, has to be overcome. It has been hindered the progress in cosmology for many decades. Our spheric universe of constant radius has all facilities to be dynamic. The local universe is the youngest and the most inhomogeneous universe, we can observe.

For illustration:
The common depiction of our local universe to be a **rubber blanket** is leastways misleading: Heavy celestial bodies hover like spheres over a two-dimensional plane grid pattern, which is dented under every celestial body proportional to its mass. This raster should represent a two-dimensional projection of the 3-dimensional space. The global curvature is neglected.
But at the **Schwarzschild model**, the grid must have a slight curvature coming from the Schwarzschild radius. These curvature may not be neglected in cosmology!
Local mass concentrations have to be depicted as **circular disks**. Their outer borders (to be drawn as a ring) represent the surface of the celestial bodies. There is a **discontinuity** between the gravitational field lines of the universe and the body, when the radius of the body exceeds its Schwarzschild radius: The angle between the circular disk and the field lines of the universe exceeds 90°. An approaching second body shatters at the surface of the first.
Initial at the changeover of a local mass to a **black hole**, the circular disk becomes a spheric body in our model. The crater in the cosmic sphere adapts **without discontinuity** to the tangent of the local spheric body. The **bigger** the black hole the slighter **are the tidal forces** in its vicinity. The passage 'into' the hole occurs nearly inappreciable without collision.
A problem for travellers might be, that the black holes exhibit their **anti-matter surface** to its outside. They are presumably 'turned inside out'!

6.1.1 Time Intervals

The limitation of the light travel time to 13.8 billion years doesn't exist in the **Schwarzschild universe**. Even the opposite pole, i.e. the place we can observe **infrared galaxies**, (chapter 6.2.1) is 44 billion (light) years away. The microwave background achieves us from the self-pole, which is 88 billion (light) years away. For the explanation of the temperature T of 2.73K there are infinite pairs of T and z, for examples: 6000K/ z~2200, 3000K/ z~1100, 1460K/ z~534, and so on.

My thesis:
I have decided on the last case, because the redshift of $z=e^{2\pi}-1=534.5$ means one circulation of light at the spheric model (2π), if the energy-loss rate per angle accounts for 1/1 to the limit value zero. One arcsecond means a redshift of $z=4.848\cdot10^{-6}$ and a distance $D_{\log}=R_U\cdot4.848\cdot10^{-6}=2.138\cdot10^{12\,m}=67745$ light years.
As described in chapter 2.11, $H_0=70$ means a time constant of the exponential function of $t_0=4.407\cdot10^{17}\,s$. Thus each photon looses $\Delta E=t/t_0=2.269\cdot10^{-18}$ of its energy per (light) second, and $\Delta E=7.16\cdot10^{-11}$ of its energy per year ($t=1\,a=3.1557\cdot10^{7\,s}$). Even for one million years, one can calculate the energy-loss, i.e. the redshift, linear ($\Delta E=7.16\cdot10^{-5}$). After one circulation around the extragalactic space, each photon looses $1-1/534.5$, i.e. more than 99.8% of its energy.

At the **standard model**, the microwave background (CMB) is a homogen radiation, which is not a superposition of the emission of single sources, in contrast to all other wave ranges; refer to (→Schneider 2008, page 379ff). This exception is omitted at the **Schwarzschild model**.

6.1.2 Voids and Filaments

One of the huge problems in the **standard universe** is the explanation of such quick and entire evacuation of empty spaces (**voids**); refer to (→Little & Weinberg 1993). The density of matter in voids comprises probably some powers of ten under the averaged density (1 H-Atom/m³) of the whole universe.

My thesis:
In the **Schwarzschild universe**, it is to assume a development, beginning many 100 billion years before the irradiation of the microwave background began. Not only the gravitational conglomeration of matter is a self-reinforcing process, but also the depletion of spaces: In voids prevails increasingly the Newtonian mechanics, due to the lack of space curvature. In voids, moving matter doesn't loose energy by gravitational waves and can leave voids without hindrance, *even matter has to leave it inevitably*. Unmoving matter in voids is situated in an unstable equilibrium, like a pencil standing on its tip. Finally those spaces are totally flat and empty (in terms of geometry).

6.1.3 Intra cluster Medium (ICM)

The ICM is extreme hot gas, dispersing in galaxy clusters. The x-ray satellite ROSAT reveals the high temperatures. (→Demarco 2003, table 1) specifies 25 galaxy clusters in our vicinity ($z \sim 0.3$) with a temperature of the ICM of $13 \cdot 10^6\, K \leq T \leq 144 \cdot 10^6\, K$

There are three problems:

1. The mechanism to effect the gas getting such high temperatures, is ascribed to magneto-hydrodynamic shock waves, although galaxy clusters are virialised, namely they should not be dynamically (→Demarco 2003).
2. Ions of the ICM having such high kinetic energy should have volatilised for longer time, similar to single galaxies of Zwicky's galaxy clusters. (→Zwicky 1933) noticed that galaxy clusters should have dissolved due to the high velocities of their members. At the standard model, the gravitational effect of non-baryonic dark matter is used to explain keeping the ICM respectively the galaxies together.
3. The inflow of the gas to the centre of the cluster and its postulated cooling flow doesn't operate like assumed. For example, the virialised gas of Abell 1835 should cool down from $80 \cdot 10^6\, K$ to nearly zero by irradiation of photons, but one observes a minimum temperature of $30 \cdot 10^6\, K$ (refer to →Schneider 2008, page 248 ff).

My thesis:

1. Micro-gravitational waves heat the ICM continuously, the thinner the plasma, the hotter, self-evident proportional to the intensity of the sources, the fusion reactors in the stars. The plasma becomes so hot, because the amplitudes of gravitational waves at each location can sum up infinitely. **Thus gravitational waves are not quantised.** At ICM, the UV-catastrophe occurs analogue to the Rayleigh-Jeans law that is attenuated by irradiation of gamma quanta in the end.
2. The ICM is held together, because each particle always looses gravitational energy in all directions, due to the thermal acceleration and due to the minimum local space curvature. Additional dark matter is not necessary to explain the cohesion of the ICM. Of course, the above-mentioned effects occur in *interstellar* media within single galaxies and also at the *corona* of our sun.
3. The gas in the centre of clusters is denser than further outside, like at every agglomeration of matter. Due to the mentioned-above mechanism (1.), the denser gas near the centre is cooler than the outer.

6.1.4 Tolman Test of Surface Brightness

Once Allan Sandage begun his scientific career as an assistant of Edwin Hubble and soon became a huge critic of Hubble. He published overall five paper, four of them with Lori M. Lubin, in there titles occur '**the reality of expansion**' (→Sandage & Lubin 2001, →Lubin & Sandage 2001a, →Lubin & Sandage 2001b, →Lubin & Sandage 2001c, and →Sandage 2009), based on data up to $z \sim 1$. But they can not reach the decline of surface brightness of celestial objects of $B \propto (z+1)^{-4}$, theoretically postulated by (→Tolman 1930). In (→Lubin & Sandage 2001c), they state that they combine their signal of surface brightness with the theoretical signal $(z+1)^{-4}$ of Tolman. They interpret the difference due to the **luminosity evolution** at 'high' redshifts. They achieve a Tolman signal in the R-band of only $(z+1)^{2.28} - (z+1)^{2.81}$ and in the I-band of $(z+1)^{3.06} - (z+1)^{3.55}$. One can contrast these results to the (wrongly) supposed luminosity evolution in the UV-band of in the range, indicated by equation 29: Lubin & Sandage 2001c argue that the strong dilution of the surface brightness is partly overridden by the steep ascent of the luminosity evolution in the range .
In contrast to Sandage, (→Lerner 2018) and (→Lerner et al. 2014) research a much wider range (up to $z \sim 5$) and conclude that there is no expansion of space in the evolution history of the universe. However Lerner et al. presume the universe to be pure euclidean. They criticise expressively the evolution of the size of spiral galaxies, including the halos of dark matter, predicted by (→Mo et al. 1998). Therefore, these galaxies ought to be distinctly denser and smaller in former days. (→Lerner 2018) determined spiral galaxies *and* elliptic galaxies to have constant size and constant luminosity over a range of $0 \sim z \sim 5$.

My thesis:
Sandage & Lubin incorporate a strong luminosity evolution into their data, similar to the data described in chapter 6.3. Therefore, there is an UV-luminosity evolution up to $-1.9\,mag$ in the redshift range of $0 \sim z \sim 1$, i.e. in former times, galaxies ought to be much brighter and the star formation rate much higher. Nonetheless, the Tolman signal of $(z+1)^{-4}$ can not be achieved by far. The signals in the R band respectively I band are not directly comparable to the UV band, but they better fit to the luminosity and the size evolution of the **Schwarzschild model**: Of course, there also is an evolution, extending to a much bigger period (> 88 billion years), and it is just contrary to the population synthesis of the standard model, described in chapter 2.10. Thus, primordial galaxies had less mass and were less dense, thereby redder, comparable with low surface brightness galaxies (LSB), described in chapter 6.2.16.

6.2 Particular Galaxies

6.2.1 Infrared galaxies

table 6: IR-galaxies: Overview

Designation at the standard model	Properties at the Schwarzschild model
LIRGs: Luminous infrared galaxies, $(L_{bol} > 10^{11} L_{\odot})$, (chapter 6.2.6).	Primordial galaxies near the opposite pole with on average redder spectral class compared to modern galaxies. Rather elliptical galaxies.
ULIRGs: Ultra luminous infrared galaxies, $(L_{bol} > 10^{12} L_{\odot})$, (chapter 6.2.6).	Primordial galaxies, often established as optical galaxies, because of their higher UV fraction. Near the opposite pole. At least two areas of light emission i.e. bulge/ disc.
HyLIRGs: Hyper luminous infrared galaxies $(L_{IR} > 10^{13} L_{\odot})$, (chapter 6.2.7).	Due to appreciation of too high redshift, they are ascribed too high luminosity. Primordial galaxies rather behind the opposite pole.
Seyfert galaxies: Galaxies with active galaxy nucleus (AGN), however obscured by dust (chapter 6.2.8).	Primordial galaxies near the opposite pole without AGN, respectively without super massive black hole (SMBH),but with a bulge in the centre.
LINER-galaxies: Low ionization nuclear emission line, also named 'starburst galaxies', many young stars, also obscured by dust (chapter 6.2.9).	Primordial Galaxies without AGN, respectively without super massive black holes (SMBH), and without a bulge in the centre. Near the the opposite pole.
HII galaxies: Dwarf galaxies. Spectrum comparable to hydrogen clouds in the Milky Way (chapter 6.2.10).	Primordial dwarf galaxies near the opposite pole.
DOGs: 'Dust Obscured Galaxies', focus of considerations on the obscuration of the energy source (chapter 6.2.11).	Primordial galaxies near the opposite pole.
EROs: 'Extreme Red Galaxies' (chapter 6.2.12)	Primordial galaxies *behind* the opposite pole, i.e. redshifts $z > 22.14$.

The launch of the Infrared Astronomical Satellite (IRAS) on 1983 and its successor, the Infrared Space Observatory (ISO) from 1995 to 1998 led, amongst others, to the discovery of infrared galaxies. Over the years, they were subdivided into several classes (refer to table 6). Among the IR galaxies, one finds the galaxy Arp 220, established since 1866, because it is

bright enough in the optical range (UV rest wave length). Most of the IR galaxies were unknown before, because their apparent luminosity is often 100 times less in the optical range than in the infrared range.

My thesis:
At IR galaxies, the immense distance of about 44 billion light years, associated with redshifts of about 22, was not realised. Due to the vicinity to the **opposite pole** of the universe, they appear in their extension as large as common galaxies of our own galaxy cluster ('ghost galaxies').
Owing to the neglected high redshifts, the apparent high ratio of infrared light are ascribed to the galaxies themselves. Thus, an abundance of additional assumptions is necessary to get a plausible model of IR galaxies at all. Some of these problems were illustrated in the following chapters.

6.2.2 The remarkable Galaxy Markarian 231

In the year 1969 Mrk 231 (= UGC 8058) became firstly well-known as a strong UV source. It was classified into Seyfert type 1 galaxies.
The distance ladder of extragalactic objects is extrapolated by comparing their spectra, by means of overlaying similar multiplets with known, weakly shifted lines (such as figure 5 in Hubble 1937). This procedure could fail, if objects of apparent other spectral lines of very different elements and ionisation levels have to be classified. Thus (→Boksenberg et al. 1977) determine for Mrk 231 on the basis of a system of emission lines a redshift of $z=0.042$, in contrast absorption lines of $z=0.021$ and $z=0.027$. They criticise the total lack of the Mg 1b and G Band absorption lines, usual in other galaxies. Therefore, they see considerable differences to otherwise comparable galaxies. (→Boksenberg et al. 1977) write in their final remark that their paper has only touched a proper analysis of the absorption lines from a physical point of view. The simultaneous presence of a sodium D-line and a hydrogen line in the systems I and II is not properly understood. Later Mrk 231 was classified to be one of the most luminous infrared galaxies (→Soifer et al. 1987).

My thesis:
In data bases for spectral lines, there are tens of thousands of spectral lines of all elements and ionisation levels. Thus, at an automatised spectrum analysis, one can always find sufficient 'fitting' spectral lines in a total different wave length range, to match more or less with the observed galaxy spectrum. For a newer paper about the difficulties to classify Mrk 231 refer to Leighly et al. 2016.

6.2.3 Identification of Redshifts by assembly line

(→Kim et al. 1995) tackle the task to find the optical counterparts of IRAS galaxies and to generate their spectra. Kim et al. register 200 galaxies and their properties. By means of the flux ratio $S_{60\,\mu m}/S_{100\,\mu m}$ 114 of them are classified as 'bright' and 86 as 'warm'. Among the bright galaxies, there are 94, which are known from other catalogues (with the identifiers NGC, MCG, UGC, Zw and ESO), among the warm galaxies only 5. There are conspicuous features at the 'forbidden' lines of oxygen [OIII] of $495.9/500.7\,nm$: 100 of the 200 galaxies have no $495.9\,nm$ line, although the $500.7\,nm$ line exist, further 20 galaxies have no [OIII] lines at all.

My thesis:
(→Kim et al. 1995) try to fit $z\sim22$ galaxies with $z\sim0$ spectra. Both [OIII] lines are found normally *together* in non turbulent and not overly dense gases. The redshifts, determined by Kim et al, constitute the erroneous basis for many following examinations.

6.2.4 Polycyclic Aromatic Hydrocarbons

(→Léger & Puget 1984) are concerned with clouds of dust and grains *within* the Milky Way. They propose huge **p**olycyclic **a**romatic **h**ydrocarbons (**PAH**s) to be sources for **u**nidentified **I**R (emission) **b**ands (**UIB**s) in the range of µm. They compare the modelled emissions spectra of Corene with those of NGC 7027 ('Jewel Bug Nebula', a planetary nebula) and HD 44 179 ('Red Rectangle Nebula', a protoplanetary nebula). They find conformity at 3.3 , 6.2, 7.6, 8.85 and 11.9 µm. Thereby is a problem to explain, how UV photons provoke infrared emissions, without disintegrating the responsible molecules or very small dust grains, and how the nearly complete transformation of UV energy to infrared is possible. Puget & Léger 1989 introduce especially the concept of 'thermal fluctuation': in diffuse interstellar medium (ISM), thermal radiation of for instance 60K should lead to a 'colour temperature' of 1000K. They regard the dust model, augmented by *compositions* of PAHs with up to 90 atoms that don't yet occur in the laboratory, has to be further confirmed. The accordance of the photometric spectra of NGC 2023 (an emission and reflection nebula in the constellation of Orion) with actual spectra of the laboratory (Corene, Circobiphenyl, Dicorene and Ovalene) are 'rather poor'.

6.2.5 Observations by ISO

Genzel & Cesarsky 2000 write concerning our galaxy that the interpretation of PAHs without an exact identification of specific molecules has been established. But the key prediction of IRAS objects could not be verified by ISO observations: The spectral PAH features should consist of a superposition of a huge number of narrow lines, affected by quantised rotational and vibration modes; this isn't observed by ISO.
Soon after the termination of the ISO mission, (→Genzel & Cesarsky 2000) provide an overview of the obtained results. By means of IRAS, one could merely undertake *photometry* in 4 IR bands. However with ISO, one could generate many IR *spectra* of 'common galaxies' and 'active galaxies'. **ULIRGs** (ultra luminous infrared galaxies, refer to chapter 6.2.6) are

assigned to active galaxies, although their nuclei often are not visible. It is postulated extreme dense shells of dust, which obscure the active galactic nuclei (AGN). Even common galaxies have IR features, which have a total different extension compared to the optical projection: Thus M31 (Andromeda, a spiral galaxy in our vicinity) has a distinct closed ring in the infrared band outlying the disc.
(→Genzel & Cesarsky 2000) conclude that 35 years after the discovery of ULIRGs and despite of the abundance of observations during decades, the central questions are clarified by no means: What dominates on average the luminosity of ULIRGs and how they evolve.

My thesis:
Due to the new classification of ULIRGs to be high redshifted ghost galaxies, many problems of the properties of such galaxies will be obsolete (refer to chapter 4.4 and →Eddington 1930).

6.2.6 Luminous and Ultra Luminous IR Galaxies

One can graduate IR galaxies on the basis of the bolometric luminosity (L_{bol}), i.e. the luminosity over the total spectrum: $(L_{bol}>10^{11} L_{\odot})$ for LIRGs and $(L_{bol}>10^{12} L_{\odot})$ for ULIRGs.

6.2.7 Hyper Luminous IR-Galaxies

(→Fan et al. 2016) introduce a subset of infrared galaxies, the hyper luminous infrared galaxies (HyLIRGs). Their luminosity amount to $(L_{IR}>10^{13} L_{\odot})$, and they ought to have one ore more obscured UV sources to explain the enormous infrared luminosity. Further, their redshift should account for $3 \sim z \sim 4.5$. (→Fan et al. 2016) give the example of the galaxy W0410-0913 with $z \sim 3.6$. In figure 7, this galaxy is recalculated to the rest wavelength at the **Schwarzschild model** (i.e. to $z \sim 20$). The red graph begins at about $300\,nm$ and ends at $100\,\mu m$. In figure 7 is also plotted the Planck spectrum of our own ancestral galaxy at the self-pole at $z \sim 534$ with $T \sim 1500\,K$ and $\lambda_0 \sim 2\,\mu m$ (blue graph). A rough calculation shows: A $z \sim 0.1$ galaxy ($D_{\log} \sim 400\,Mpc$), to be classified as a $z \sim 3.6$ galaxy ($D_{\log} \sim 6.5\,Gpc$), is overestimated 500-times of its luminosity. Similar are the overratings to the complementary locations ($z \sim 20$ / $D_{\log} \sim 13\,Gpc$) and
($z \sim 24.5$ / $D_{\log} \sim 13.9\,Gpc$) of the $z \sim 0.1$ galaxy, before/ behind the opposite pole.
The overestimations are about 300- times and 250-times. Hence W0410-0913 is not much brighter than other IR galaxies. Complementary locations refer to chapter 6.2.14.

My thesis:
HyLIRGs are common, but primordial galaxies near the opposite pole to be as far as possible virialised, in contrary to Arp 220 (yellow graph in figure 7). They have no ostentatious optical and UV sources in contrast to Arp 220 to be detected in the optical range. The first maximum at rest wavelength range 10 to 100nm arrives the observer at 230 to 2300nm.)
For the spectrum of a 'DOG', shown in figure 7, neither highly dust-obscured energy sources, nor dust are necessary at all. The stars of W0410-0913 and similar galaxies are just smaller and redder on average than in modern galaxies.
Most likely, the Planck spectrum at $T \sim 1500\,K$ of our ancestral galaxy is not the entire spectrum. Further spectral fractions could be masked by the overall cosmic background radiation, extending over 20 decades from radio sources to gamma rays (for example refer to →Schneider 2008, figure 9.24, page 379).

6.2.8 Seyfert Galaxies

The energy source, provoking the high infrared luminosity of the galaxy, is ascribed to an active galaxy nucleus (AGN), which is obscured by dense dust.
Essentially, an AGN is a **super massive black hole** (SMBH) in the centre of a galaxy that collects a lot of matter in an accretion disc. For most of the part, this matter is transformed to radiation energy by gravitational forces. An extreme dense dust shell is postulated hiding the AGN, which isn't visible in IR galaxies.

My thesis:
Generally speaking, the inner dynamics of galaxies is very similar, regardless of a SMBH in the centre or not. Seyfert IR galaxies are primordial, but in other respects quite common galaxies near the opposite pole, 40 to 50 billion years ago. Therefore, a black hole had not formed until that time, at any rate no SMBH.

6.2.9 LINER and Starburst Galaxies

'LINER' stands for 'Low Ionisation Nuclear Emission Line Region' that are galaxies to have emissions lines of low ionisation level in its centre region, on the contrary ascribing them a high energy density. If the energy source is not concentrated in the centre of the galaxy, but is scattered all over the galaxy, it is named 'starburst galaxy'. It is assumed to have a lot of UV bright stars that are not visible directly. These young stars are also dust obscured, and there is a high star formation rate.

My thesis:
To explain IR luminous LINER and starburst galaxies, one needs no UV bright stars to be obscured. These galaxies are primordial galaxies at the opposite pole of the Schwarzschild universe, redshifted by $z \sim 20$.

6.2.10 HII Galaxies

HII galaxies are bright IR dwarf galaxies, to be compared in respect of their spectra with HII regions in our Milky Way. At the standard model, they are equalised with starburst galaxies, refer to chapter 6.2.9.

6.2.11 Dust Obscured Galaxies

Dust Obscured Galaxies ('DOGs') to have comparatively low dust temperatures, compared to HyLIRGs. Dust Obscured Galaxies with higher dust temperatures are named 'Hot DOGs', refer to chapter 6.2.7

6.2.12 Extremely Red Objects

The apparent brightness of Extremely Red Objects (EROs) constitutes in the $K_S-band<20$, i.e. in a window of the earth's atmosphere at about 2µm. So it can be determined by earth bonded telescopes. Actually, they should be named 'Extremely *Infrared* Objects'.

My thesis:
The example of chapter 6.2.7 shows: Galaxies with distances of $D_{\log}\pm 400\,Mpc$ before and behind the opposite pole at ($z=22.14$) differ in their redshift in $z\approx\pm 2.5$, not only in $z\approx\pm 0.1$, compared to the local universe. Galaxies behind the opposite pole appear on average (infra-) redder and have an earlier stage of development at similar amplification factors.

6.2.13 ULIRGs in the Local Density Field

Dekel 1994 deals with the density of galaxies in the local universe. His issue is the likelihood to find one or more additional galaxies in a well defined vicinity of an examined galaxy. Dekel determines this separately for normal and infrared galaxies, mapped to the supergalactic plane. The result of density fields are velocity fields and reciprocal. Figure 8 shows the pigmented, scaled and layered figures 4a and 4b of (→Dekel 1994) within a radius of 112 Mpc.
The red layer represents the velocity vectors of IRAS galaxies $\vec{a}$, and the blue layer those of normal galaxies $\vec{b}$. 738 pairs of vectors ($\vec{a},\vec{b}$) can be found.
To get an index of correlation, one has to calculate for $|\vec{a}|\leq|\vec{b}|$:

$$r_{ab}=\frac{|\vec{a}|}{|\vec{b}|}\cos(\sphericalangle\vec{a},\vec{b}) \quad . \qquad (32)$$

For $|\vec{a}|>|\vec{b}|$, one has to calculate:

$$r_{ab}=\frac{|\vec{b}|}{|\vec{a}|}\cos(\sphericalangle\vec{a},\vec{b}) \quad . \qquad (33)$$

The arithmetic mean of all $-1<r_{ab}<+1$ of all 738 vector pairs is the overall correlation and yields 0.34. For an autocorrelation, one has to built vector pairs between each vector and its next two vectors, separated by columns and rows, and separated by IRAS and normal galaxies. There a further $4 \cdot 707$ pairs of vectors, with the averaged correlation numbers of 0.77, 0.80, 0.83 and 0.83. These numbers clearly comprises below one, but significantly above 0.34.

My thesis:
Normal galaxies and ULIRGs are not gravitationally bonded, because their vicinity is merely apparent. The best explanation is that ULIRGs are strong lensed ghost galaxies, and they are on average 44 billion light years away from the local universe, namely near the opposite pole.

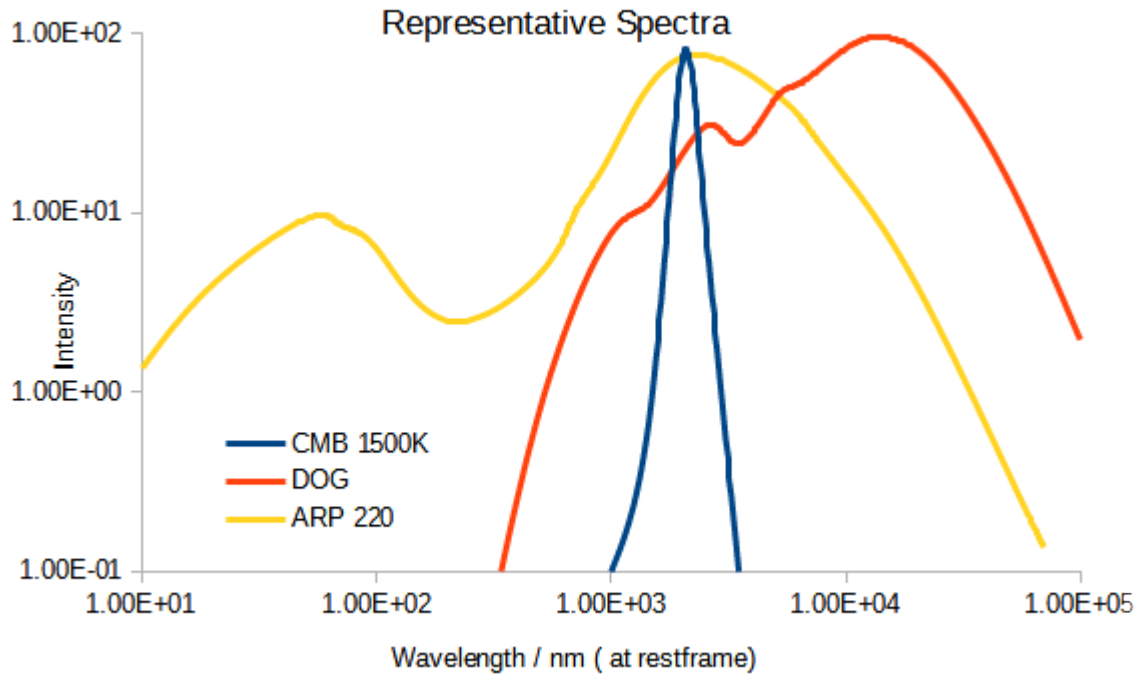

Figure 7: Comparison of different celestial objects at rest frame

6.2.14 Complementary Locations near the Opposite Pole

Assuming that the above mentioned galaxy Arp 220 wasn't 250 million light years away from us, as nowadays commonly accepted, i.e. at $z=0.0183$, but accordingly 250 million light years before and behind the opposite pole of the Schwarzschild universe that is located on a distance of 44.38 billion light years at $H_0=70$. So one gets the following relations for the redshifts: $(22.5648+1)/(22.1407+1)=(22.1407+1)/(21.7248+1)=0.0183+1$, where $z=22.5648$ is the redshift behind the opposite pole, $z=21.7248$ the redshift before the opposite pole and $z=0.0183$ the to date's accepted redshift of Arp 220. $z=22.1407$ is the redshift just at the opposite pole, determined in this paper. Its redshift is independent of the accurate size of the Schwarzschild universe. For the corresponding distances $D_{\log}$ at $H_0=70$ is valid: $44.14-43.88=43.88-43.63=0.25$, all distances in billion light years. These three locations ($44.14/43.63/0.25$ billion light years) are complementary, because they have the same aspect ratio to the observer. $D_{\log}=43.88\,Glyr$ is the logical distance just at the opposite pole, determined in this paper.

6.2.15 Duplicated images

Asymmetric double images of gravitational lensed quasars can have time delays of several month between each other. Infrared galaxies have also two projections, one of them by light rays propagating directly from the place before the opposite pole to the observer, the other projection by light rays, passing firstly the opposite pole to cover then the distance of the 'remaining' 44.38 billion light years. Generally, the time difference of those two images should amount many million years !

My thesis:
Arp 220 could be a primordial galaxy near the opposite pole of the Schwarzschild universe. There are always two images with the same aspect ratio of any IR galaxy respectively. The projections are mirror inverted to each other and their difference in lapse of time comprises in our example $2\cdot 0.25\,Glyr$. Thus, twin-projections are difficult to find and to recognise to be twin-projections!

6.2.16 (Giant) Low Surface Brightness Galaxies

Malin 1 is perhaps the biggest member of **giant low surface brightness galaxies** (GLSBs), firstly described by (→Bothun et al. 1987). This galaxy is in contrast to its size $R\sim 200\,kpc$ at $z=0.083$ not detectable by earth bonded telescopes, because the surface brightness of its disc is dimmer than the surface brightness of the earth's night sky. It is rated as HI-gas-rich, with a mass of $(5\cdot 10^{10}\,M_\odot)$ that fits actually to its luminosity of $L\sim 5\cdot 10^{10}\,L_\odot$. But it is presumed to be eminently massive with $10^{12}\,M_\odot$, calculated by the gradient of its rotational velocity curve. This means that it has a 20 times fraction of dark matter according to the standard model (refer to →Barth 2007).

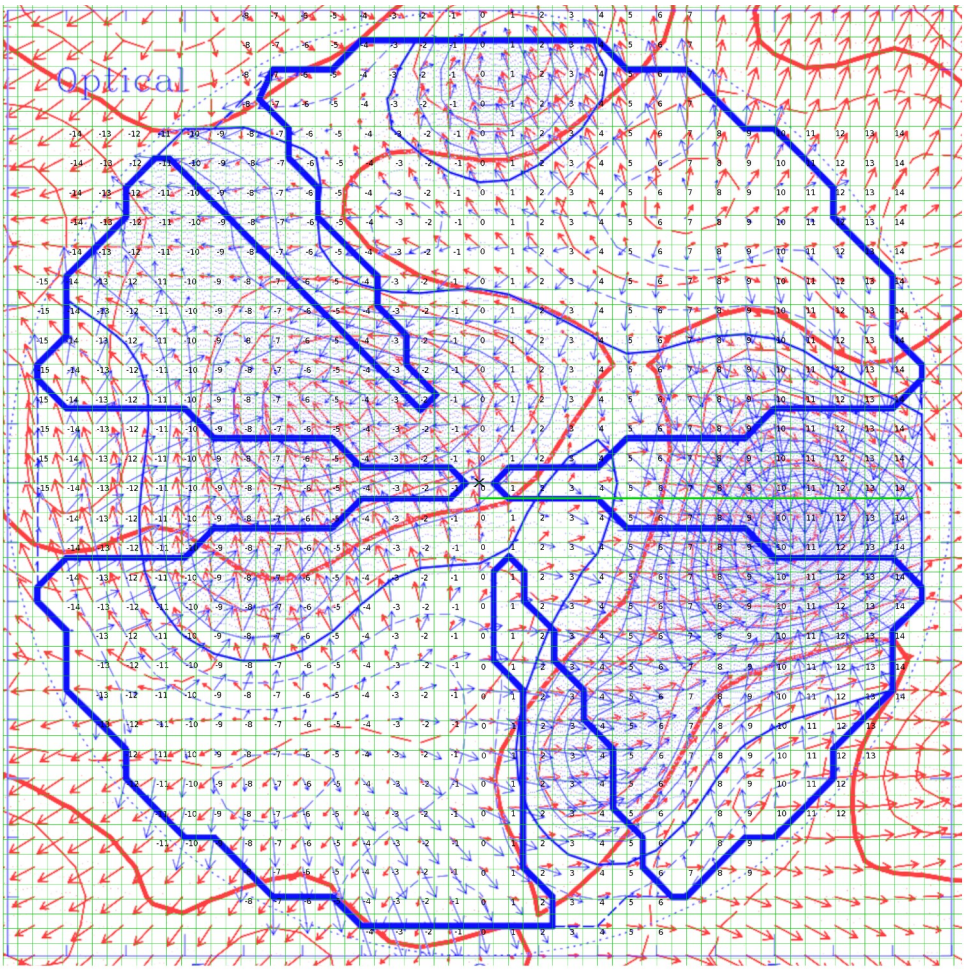

figure 8: Combined fluctuation fields of velocity in the local universe

Whereas (→Rosenbaum et al. 2007) research the large-scale allocation and number density of smaller low surface brightness galaxies (**LSBs**), in comparison to high surface brightness galaxies **(HSBs)**. They discover that LSBs occur much rarely than HSBs. LSB are often found on the fringes of voids or even in voids, i.e. their location of origin. The precise physical mechanism is difficult to understand according to (→Rosenbaum et al. 2007).

My thesis:
Malin 1 reside in a transition area of a void to a filament. At the **standard model**, the observed kinetic dynamics is ascribed to a huge amount of dark matter. In the **Schwarzschild universe**, the considerably increased curvature of space at a transition area void to filament is the reason of the kinetic anomaly of LSBs.
The origin of Malin 1 is evidently a depleted environment, with a curvature of space of nearly zero (i.e. a void). The marginal losses of energy by gravitational waves effectuated a much slower shrinking, compared to other galaxies (i.e. HSBs). In the low density of matter, the progenitor of Malin 1 could collect only a small amount of gas, and became an elliptical galaxy with comparatively poor amount of matter. The current collision with the

border of the filament, nowadays promotes the formation of bigger stars with higher UV luminosity. Thereby, it is drawn apart to a spiral galaxy.

Summary of chapter 6.2.16:

LSBs generally are low-mass elliptical galaxies in voids, not yet approaching the rims of the filaments. The star formation rate is still very low. The motion of single stars resemble the **Newtonian Dynamics**, due to very low space curvature.
GLSBs are just influenced by the matter of the nearby filament, drawn apart to spirals, and captured by the increasing curvature of space in filaments. Thereby, the star formation rate and the opportunity to gather matter also increases.
HSBs emerge from the beginning inside of filaments and have an advantage of number density, mass, and stage of development, compared to **(G)LSBs**.

6.3 Reversed Luminosity Evolution

(→Bruzual & Charlot 1993) determine a distinct spectral evolution at star clusters of the same age. They see specific variations of the colour magnitude diagrams over the redshift range of $0<z<1.2$, i.e. over 12 billion years. They find evidence that stronger redshifted cluster have a higher star formation rate. They conclude that clusters in our vicinity have burned out distinctly their nuclear fuel to produce new stars. They also have to assume **initial mass functions** that are rich in massive stars, as mentioned in chapter 2.10.
(→Lilly et al. 1996) pick up the subject about galaxies of low luminosity, gauged in the 'Canada-France Redshift Survey'. They see in 3 spectral ranges (280, 440, and 1000 nm) an explicit, but different intense ascent of the luminosity of low-luminosity galaxies by increasing redshift at the range of $0<z<1$.
(→Parsa et al. 2015) deliver the most substantial meta-study till this date, about the distribution in space and luminosity of galaxies. Besides own date of redshift and luminosity of 720 galaxies, they compile further data of more than 120 000 galaxies at the range $1.5<z<4.5$ of other surveys. Data of 92 100 galaxies solely are derived from (→van der Burg et al. 2010). Further studies deliver data at the redshift range of $0<z<8$. Parsa et al. examine the UV rest frame spectral range of 150nm to 170nm that is presumed to be a good indicator for the star formation rate, because this light is radiated by mass-rich and therefore short-living stars. Moreover, one can comfortably observe UV light at the optical range, redshifted at z >1.5. Parsa et al. apply a characteristic value M^* for the absolute luminosity of galaxy populations of rather different luminosity.

Table 7: Publications compiled by Parsa et al. 2015

publication	Arxiv.org number	binned redshifts z
Hathi et al. 2010	1004.5141	2.1, 2.7
Sawicki & Thompson 2006	0605406	1.7, 2.2, 3.0, 4.0
van der Burg et al. 2010	1009.0758	3.0, 4.0
Bouwens et al. 2014	1306.2950	3.8, 4.9, 5.9, 6.8, 8.0
Bouwens et al. 2007	0707.2080	5.0, 5.7, 5.9
Bouwens et al. 2011	1006.4360	6.8, 8.0
Yoshida et al. 2006	0608512	4.0
Finkelstein et al. 2014	1410.5439	4.0, 5.0, 6.0, 7.0, 8.0
McLure et al. 2009	0805.1335	5.0, 6.0
McLure et al. 2013	1212.5222	7.0, 8.0
Ishigaki et al. 2014	1408.6903	7.0, 8.0
Atek et al. 2014	1311.7670	7.0
Schenker et al. 2013	1212.4819	7.0, 8.0
Ouchi et al. 2009	0908.3191	7.0
Schmidt et al. 2014	1402.4129	8.0
Braedley et al. 2012	1204.3641	8.0
Oesch et al. 2007	0706.2653	5.0
Arnouts et al. 2005	0411391	0.3, 0.5, 0,7, 1.0, 2.0, 2.7, 3.0
Weyder et al. 2005	0411364	0.05
Reddy & Steidel 2009	0810.2788	2.3, 3.05
Alavi et al. 2014	1305.2413	2.0
Sawicki 2012	1108.5186	2.2
Weisz et al. 2014	1409.4772	0.75, 1.25, 2.0, 3.0, 4.0, 5.0
Oesch et al. 2010	1005.1661	1.7
Bowler et al. 2014	1312.5643	5.0, 6.0, 7.0
Parsa et al. 2015	1507.05629	1.9, 2.8, 3.8
(26 publications)		(62 data points)

This method has been elaborated by (→Schechter 1976). Parsa et al. combine their own three binned data points for M^* of galaxy clusters at the range of $1.9<z<3.8$ with 59 further data points of other surveys in a M^*-z -diagram (refer to →Parsa et al. 2015, figure 10, in the middle, similar to figure 9).

They delineate a regression curve with an absolute luminosity at z=0 of $M^*=-17.7$:

$$M^*=2\cdot(-17.70)\cdot\frac{(z+1)^{0.524}}{1+(z+1)^{0.678}} \qquad (34)$$

This equation has no special physical meaning. I could find a second regression curve with slight different parameters (equation 35) that delivers the same standard deviation as equation 34. Equation 35 has a higher initial luminosity of –18.12, attenuating the luminosity evolution. This makes it easier for me to argue in favour of the Schwarzschild universe. Thus I prefer:

$$M^*=2\cdot(-18.12)\cdot\frac{(z+1)^{0.476}}{1+(z+1)^{0.633}} \qquad (35)$$

To transform the data points or the graph of equation 35 from the standard model to the Schwarzschild model, one has to apply the method described in chapter 5.9 and 5.10. For instance for $M^*=-20.33$ of (→Arnouts et al. 2005) at z=2 ($k_{sum}=-1.92$) is transformed to $M^*=-18.41$, and $M^*=-20.73$ of (→Finkelstein et al. 2014) at z=4 ($k_{sum}=-2.94$) is transformed to $M^*=-17.79$. Generally, the luminosity is estimated to be dimmer after transformation.

My thesis:
At the range of 0<z<2, one has a nearly constant UV luminosity M^* of –18.4 after transformation to the **Schwarzschild model**. That means a time period ΔD_{log} of about 15 billion years. The vast constant UV luminosity M^* of galaxy clusters at the range of 2<z<8 changes by a transformation to the Schwarzschild model to a steady decline from von –18.4 to –16.0 with lookback time. This is also a further development period ΔD_{log} of about 15 billion years.
Thereby one should consider: There are only 5400 galaxies (4.5%) at the range of 0<z<2 of over 120 000 examined galaxies! The 'change' of luminosity evolution could be caused by our random position in the universe, becoming more and more inhomogeneous with time. One can see it by the split of the data points in two stands. By means of the improved computational power nowadays, it is easy to vary the observer's place and the evolution rate virtually within the 120 000 galaxies, to generate many M^*-z -diagrams. So one can arrange a contention between Standard and Schwarzschild model.

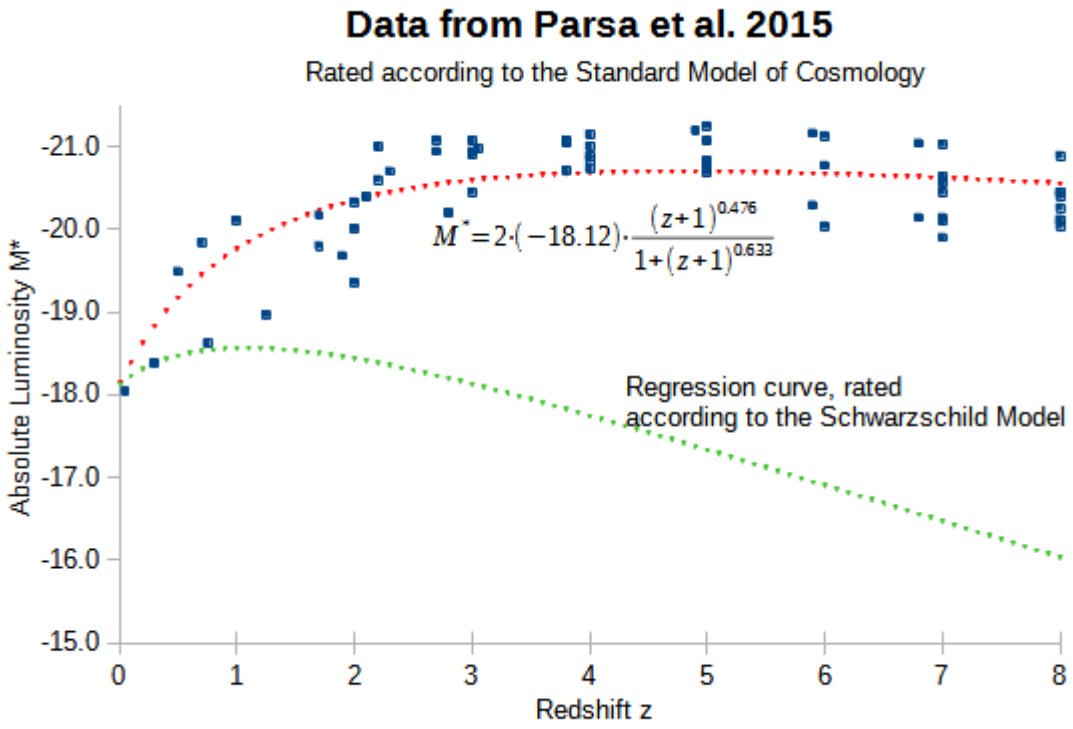

Figure 9: Standard UV Luminosity Evolution of galaxy clusters

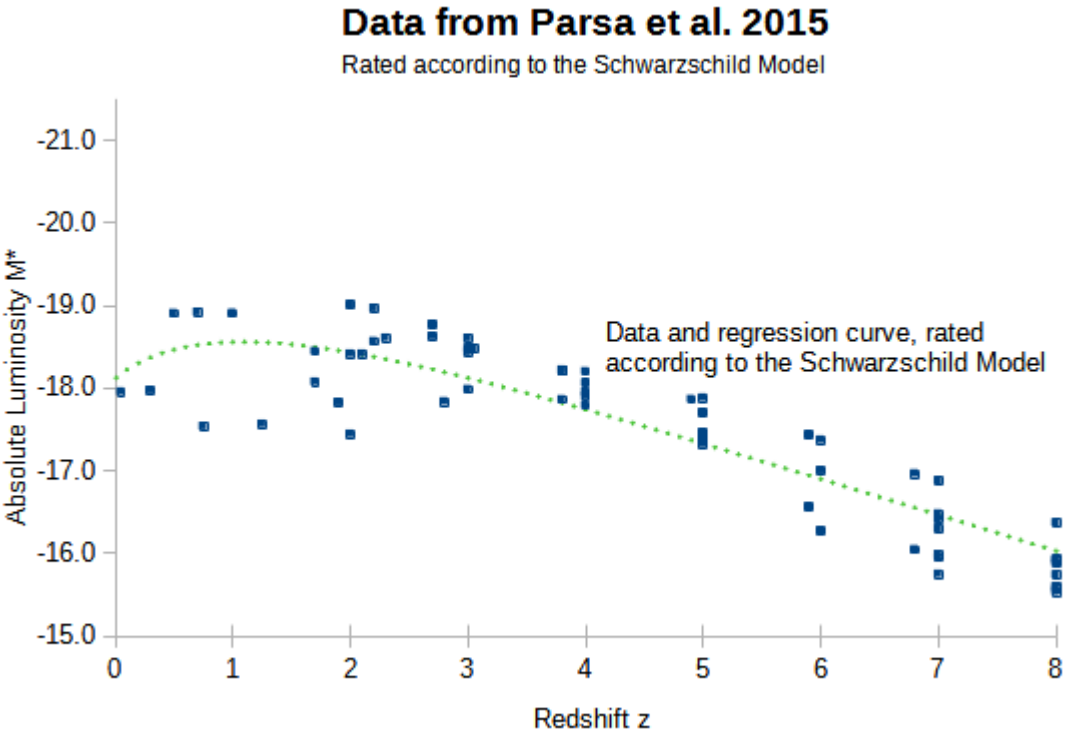

Figure 10: Reversed UV Luminosity Evolution of the same galaxy clusters

6.4 Supernovae: Suitable for Standard Candles

Supernovae of type 1a (SNe1a) are considered to be standard candles, due to their rather constant maximum brightness of their light curves. So they are suited for high-z distance measurements. But (→Phillips 1993) show by means of nine nearby SNe1a that there are bigger deviations in the maximum brightness, even in the same host galaxy. (→Gilfanov & Bogdan 2010) have an explanation of their high variability. They show that only 5% of SNe1a happen by gradual accretion of hot material on a white dwarf. Most of the SNe1a are merger of two white dwarfs, and therefore brighter than the former. The maximum brightness of the light curves correlate inversely proportional with the decay time.

(→Jha et al. 2007) affirm this on the basis of multicolour light curves. (→Kowalski et al. 2008) examine 307 of 414 SNe1a from the compilation named 'Union'. They presume their light curves to have a rather constant maximum brightness.

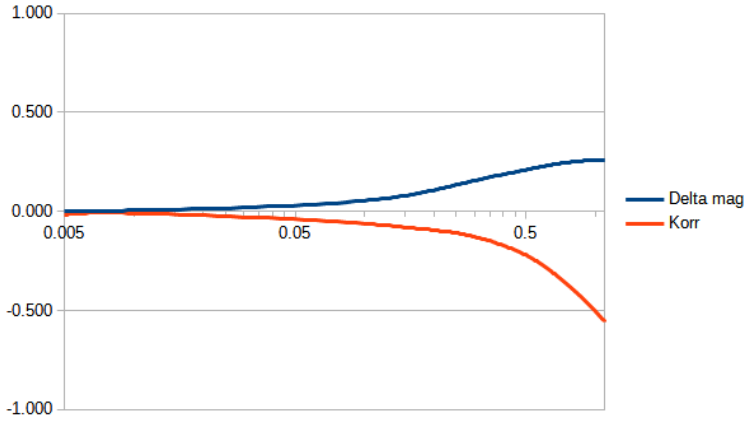

figure 11: Accelerated expansion

(→Kowalski et al. 2008) firstly compare light curves of nearby SNe1a $(z \sim 0.2)$ with farther $(z \sim 1.0)$,and they find a increasing elongation of the light curve duration, proportional to the redshift. The observed time lapse are converted to the rest frame by $t_r = t_{obs} \cdot (s(z+1))^{-1}$ at the **standard model**. The deviation from an ideal light curve duration is outsourced to a time scale stretch s that amounts on average 1.0.

(→Riess et al. 1998) has interpreted this as evidence for the cosmological time dilation $\Delta t \simeq (z+1)$ by space expansion that lapse is even accelerated, illustrated in fig. 11 by the blue plot. The upward deviation of luminosity from the baseline at z>0.05 is interpreted as an increased distance of SNe1a.

The uprising of the blue plot disappear by application of the transformation factors $k_{\log}$, k_{lum} and $k_{\sin}$ and inverts to the opposite: The maxima of SNe1a light curves get more and more dimmer with distance (refer to fig. 11, red plot). So one has to find other explanations for both effects, namely observed time dilation and decreasing maxima of the light curves.

(→Crawford 2009) searches for evidence for a 'static' universe. He postulates that the selection of light curves with equal maxima, according to the **standard model**, leads to light curves with dimmer absolute maxima at higher redshifts. Corresponding to Crawford, one has to consider the *overall energy*, i.e. the maximum brightness multiplied by the duration of a light curve should be widely constant. Expressed by logarithms, the energy $\log E = M + (-\log t_{obs})$ is nearly constant, not the maximum brightness. According Crawford, the bias to the lime lapse is caused by the selection of wider light curves with redshift at the

standard model.
Crawford proposes that different maximum brightnesses and different declining times are due to variable density of the surroundings of SNe1a. For transformation to the **Schwarzschild model** by logarithms, one can subtract the logarithm of the duration and a constant number. Thus one gets consistent values of the overall energy of SNe1a light curves in our vicinity, compared to high-z SNe1a.

My thesis:
I don't share the opinion of Crawford that there are appreciable bias at SNe1a. The bigger differences of the maximum brightness of SNe1a even at similar redshifts are real, but also the spreading of the measured values (refer to →Riess et al. 1998, fig. 4 with error bars). As described by (→Gilfanov & Bogdan 2010), brighter SNe1a can occur by *merging* of a second celestial body of about $0.1 < M < 1\,M_{\odot}$, instead of collecting material by an accretion disk. The significant value for the standard candle is the *integrated overall energy* of the light curve, as proposed by Crawford. The observed (stretched) time lapse of the light curve of SNe1a with increasing redshift is not real in the **Schwarzschild universe** and needs a new explanation: At *transient incidences,* the **cosmolensing effect**, described in chapter 4.4, produces less or no amplification of the m*aximum brightness*. In fact, the additional collecting of light rays with longer transition time provoke an *apparent* time stretch, compared to the rest frame of time lapse. At common gravitational lensing, one can observe asymmetric multiple projections of one quasar with differences in the time lapse (refer to chapter 6.2.15). At projections of high-z supernovae, one can find 'intrinsic' multiple images of one expanded light source. The variation of the observed light signal over many days is widened with increasing distance or redshift. The apparent peak amplitude is *hardly* respectively *not* increased by cosmolensing.

For illustration:
The scattering of rectangular signal slopes is well known in optical fibres to transmit digital signals: Light rays don't propagate parallel in the optical fibre, but meander due to reflections at the outer envelope. Thereby, differences of the transit time occur. The rectangular pulses are not only attenuated with increasing length of the light conductor, but get bell-shaped curves that must be amplified and reshaped after regular long-distance intervals.

6.5 Quasars

6.5.1 Overestimated Luminosity

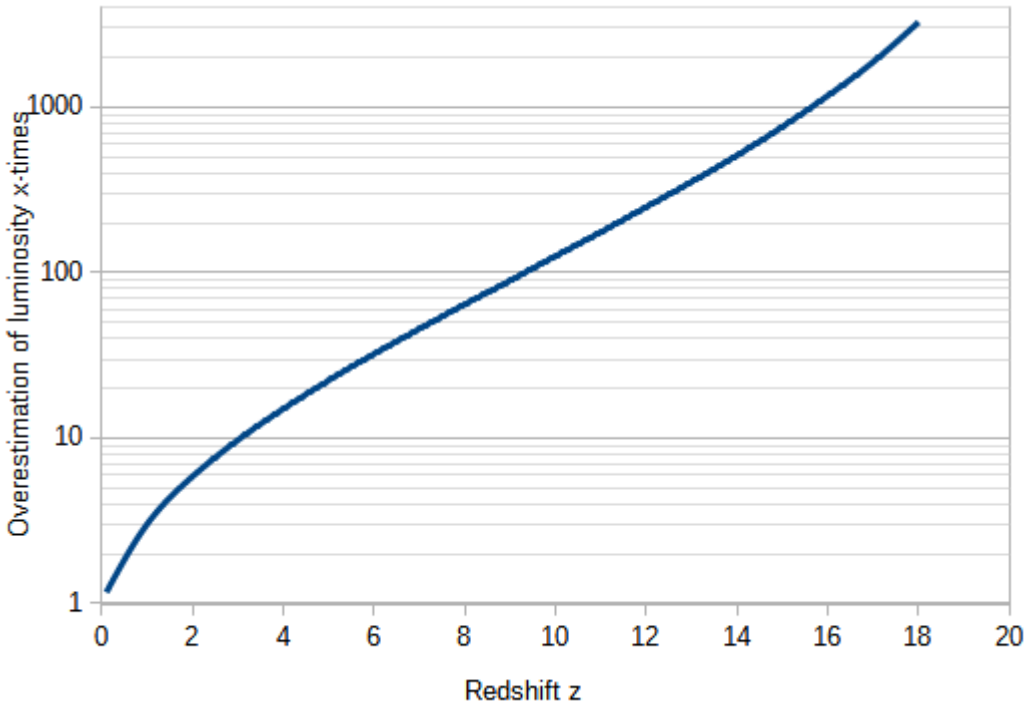

Figure 12: The luminosity of quasars are highly overestimated at the standard model

Quasars are the most luminous compact objects in the universe. (→Onken et al. 2021) examine ultra luminous quasars in the redshift range of $4.0 \sim z \sim 5.5$. For example, the quasar J165 333.86-761 426.1 has a redshift of 5.51 and an absolute magnitude M_{145} of -28.43 , rated by the standard model. This means over $10^{13} L_{\odot}$ in the UV spectrum! In figure 12, one gets an overestimation factor of 26. As a second example serves J032 233.76-594 328.1 with z= 4.42. The overestimation comprises all the same ~18-times.

My thesis:
At the **standard model**, the diluting effect of the redshift is overestimated and the cosmolensing effect is neglected. Thus, the determined absolute magnitudes of quasars often exceed the energy of the Eddington limit of accreting material by black holes. The problem is tightened by assigning too small diameters to the quasars, as described in chapter 6.5.4. The absolute diameters of the two examples mentioned above are underestimated by about three. Corrected by the **Schwarzschild model**, one gets more realistic values for ultra luminous quasars.
On the contrary to the transient light signals of supernovae (refer to chapter 6.4), the cosmolensing effect causes the full amplification of the continuous light signals of quasars.

6.5.2 Gas Clouds are not Elongated

Hennawi et al. are concerned with apparent twin-quasars, i.e. with quasars, having incidentally an transverse distance of a few arcseconds, but having considerable different redshifts (→Hennawi et al. 2006a, (HEN1) for short, and →Hennawi et al. 2006b, (HEN2) for short). By means of their high radiation power, quasars ionise their vicinity that have hence a much higher UV flux density compared to the common UV background. The light of background quasar with higher redshift trans-radiate the concentrated and highly ionised gas cloud of the foreground quasar. Self-evident the angular distance $\Delta\theta$ of the twin-quasars has to be smaller than the traverse extent R of the gas cloud in the foreground. On the basis of strength, wavelength and width of the absorption lines, (HEN1) determine the traverse extent and the density of the clouds of 27 foreground quasars. Further, they determine the length in line of sight of the clouds. Thereby, they conclude that the ionised clouds are by no means spherically, but much longer in the direction to the observer than orthogonally to this. The ratio length to width can amount more than 10, and it is strongly raised in (HEN1). (HEN2) circumscribe these peculiarities of the ionised clouds around quasars to be 'highly anisotropic' in their dimensions, without underlining the unexplainable feature that all clouds point to the observer!

In (HEN1, table 1) are 27 twin-quasars, therefrom only a selection of 17 quasars with a higher gas density of HI in (HEN2, table 1). In each column 4, one can find the radius R, i.e. the traverse dimension of the individual clouds. Thereby, (HEN1) calculate the dimension ' R ', including the feature of the standard model that the projections of the angular dimensions expand with the space. On the contrary in (HEN2), the observed dimension ' R_{obs} ' is listed without expansion. Thus, the traverse distances are increased by (z+1) in the second paper (refer to chapter 5.6, Angular Distance D_A).

My example is SDSSJ0225-0739, i.e. the quasar at the 4. line of (HEN1, table 1) and at the first line in (HEN2, table 1). For calculating D_A , one has to take the redshift of the foreground quasar ($z_{fg}=2.440$) to determine $R=1251\,h^{-1}kpc$ in (HEN1), and $R_{obs}=4310\,h^{-1}kpc$ in (HEN2), i.e. $R_{obs}=R\cdot(1+z_{fg})$ '. The overall result is that the elongation of the clouds are moderated by increasing the traverse extent of the clouds by $(1+z_{fg})$. But the elongation is not suspended by far.

In my analysis, I have omitted 3 further outliers: SDSSJ0239-0106, SDSSJ0256+0039 and SDSSJ1213+1207: The averaged elongation of the hydrogen clouds of the leaving 14 quasars is diminished from 12.17 to 3.58 by omission of the space expansion, practised in (HEN2).

The second impact to the elongation should be the linear Hubble law $H_0\cdot D_H=c_0\cdot\Delta z$ that Hennawi et al. apply for all foreground redshifts in both papers.

Applied to SDSSJ0225-0739, i.e. ($\Delta v=690\,km\,s^{-1}$), one gets $\Delta z=0.0023$ and the Hubble distance $D_H=6.9\,Mpc\cdot h^{-1}$. At the **Schwarzschild model**, one has to determine two separate logical distances, and calculate the difference:

$\Delta D_{\log}[z_{abs}+\Delta z]-D_{\log}[z_{abs}]$ at $z_{abs}=2.4476$, and with concrete numbers:

$\Delta D_{\log} = 3712.5\, Mpc \cdot h^{-1} - 3710.5\, Mpc \cdot h^{-1} = 2.0\, Mpc \cdot h^{-1}$, i.e. only 29% of D_H.
Hennawi et al. use the parameter 'h' to outsource the uncertainty of the Hubble constant: The meaning of $0.5 < h < 1.0$ is $50 < H_0 < 100\, km/s/Mpc$, an usual practice in the 20. century, not to make a commitment to an accurate number of H_0. So, one has to insert $c_0 = 3 \cdot 10^5\, km/s$ and $H_0 = 100\, km/s/Mpc \cdot h^{+1}$ into the linear Hubble law, to get $D_H = 6.9\, Mpc \cdot h^{-1}$.

My thesis:
At the **Schwarzschild model**, the linear Hubble law $H_0 D_H = c_0 z$ is valid for $z \ll 1$, but *not* for $\Delta z \ll 1$ at *higher redshifts.* Applying the latter at high redshifts, the differences of distances in line of sight are strongly overestimated. Thus the oddity of Hennawi et al. are solved. The elongation of the 14 hydrogen clouds are diminished on average from 3.58 to only 1.13, i.e. in the scope of uncertainties of measurements, they have nearly globular shapes.

6.5.3 Metallicity higher than expected

Fan et al. 2001 deal with three quasars with redshifts $z \geq 5.8$. They record spectra, determine the luminosity, and the fractions of elements beyond helium, the so called metallicity Z.
A redshift of 6 means to be one billion years after Big Bang, according to the **standard model**. Finding a metallicity that is a multiple of the sun's metallicity $Z_\odot < Z < 10 \cdot Z_\odot$, is hardly to explain. Fan et al. assume a '**top-heavy initial mass function**' (IMF), i.e. a emergence of heavy stars and even Black holes simultaneous with the Big Bang (also refer to chapter 2.10, population synthesis).

My thesis:
In the **Schwarzschild universe**, quasars with $z \sim 6$ are 16.7 billion (light) years away from the opposite pole and 60.6 billion years from the self-pole. In this period, stars had been existing, providing nuclear fusion and ejecting 'metals', thereby becoming more and more bigger. There was enough evolution time to give rise to black holes, and even to active galactic nuclei. Computer simulations will show that the high metallicity of high-z quasars can emerge offhand.

6.5.4 No Cosmological Time Dilation

Light curves of quasars are variable, but entirely incidentally. Therefore, they have to be analysed by the mathematical method of stochastic. Observational data of 190 quasars at the range of $0.2 \sim z \sim 4$ of over 20 years are available. (→Lewis & Brewer 2023) show that the variations of light curves are obviously dilated with increasing redshift. One can observe luminosity variations at the range of days and weeks, which has nothing to do with the redshift of single photons. Lewis & Brewer 2023 interpret their results to be strong evidence for

cosmological time dilation. They determine a proportional factor lying *over* $(z+1)^1$, namely $(z+1)^{1.28}$!

My thesis:
In the **Schwarzschild universe**, there is the **intrinsic cosmolensing effect**, described in chapter 6.4 on supernovae. The ratio of higher frequencies of stochastic light curves are stronger damped than lower frequencies, proportional to the distance of the quasars.
I propose a test for the Schwarzschild model, if there is a lower limit for the light curve spectra of nearby quasars: If the lower limit also is shifted to lower frequencies with increasing redshift, one should prefer the time dilation, otherwise the non-expansive model.

6.6 Anomalies of Motion

To simplify the field equations of the general theory of relativity, (→Einstein 1917) and (→Schwarzschild 1916) assume a space without curvature ad infinitum to examine *local* mass aggregations. They are aware to a non-curved space to be absolutely empty. It is 'degenerated'. Einstein assume firstly that the universe is closed and spherical and state the equation $V_U = 2\pi^2 R_U^3$ for the 3-dimensional surface of a 4-dimensional hyper-sphere ('static' universe).

My thesis:
The discrepancies of an expansive universe are not solved and the anomalies to the Newtonian dynamic are gilded more and more with additional assumptions (parameters). All the inadequate explained 'anomalies' of cosmology can be solved by consequently applying the physics of Einstein, summarised in this paper on the **Schwarzschild universe** and its facilities of evolution.

6.6.1 Spiral Galaxies and MOND

The rotational curves of the discs of spiral galaxies are expected to respond to the Keplerian velocity-distance law $v \propto r^{-2}$, like the orbital motions in our solar system. (→Babock 1939) undertakes elaborated measurements of the rotation of the Andromeda galaxy (M31). He determines a circular velocity increasing with radius and a nearly constant angular velocity. On the contrary to the decreasing surface brightness with increasing radius, he calculates by gravitation an increasing mass fraction. He determines a total mass of M31 to $1.02 \cdot 10^{11} M_\odot$ and a luminosity of $2.1 \cdot 10^9 L_\odot$, thus a ratio of mass to luminosity of $M_\odot / L_\odot \sim 50$, for Babock an indication to a high amount of mass being invisible on the photographic plates.
Vera Rubin and Kent Ford pick up the issue more detailed (→Rubin & Ford 1970). In their paper (figure 15), they plot the revolution velocity of M31, not rising at the outskirts at 9.5 kpc corresponding to Babock, but falling at a radius of 24kpc from ~ 260km/sec to ~200km/sec. This rotational curve neither corresponds to the Keplerian law by far. So Rubin and Ford also

presume an increasing amount of invisible matter with radius at M31.
In 5 publications until 1978, Rubin et al. determine rotational curves of 15 further spiral galaxies that rather have a horizontal than a quadratic declining characteristic velocity-to-radius curve (refer to →Rubin et al. 1978 and associated papers).
Mordehai (→Milgrom 1983b) detects that one needs no dark matter, if one assumes an universal acceleration constant of $a_0 \approx 4 \cdot 10^{-10}\, ms^{-2}$ (at $H_0 = 70\, km\, s^{-1}\, Mpc^{-1}$). That constant should provoke an additional small acceleration in direction to the centre of gravitation at small centrifugal forces. At this limit value of a_0, there should remain a minimum acceleration deviating from the Newtonian gravitational law. Thus this law is modified, therefore the name '**Mo**dified **N**ewton **D**ynamics', for short '**MOND**' arises (refer to → Milgrom 1983a and his subsequent papers). Meanwhile Milgrom has published dozens of papers to show by means of very different objects in the universe that MOND can predict their motions, without the help of arbitrary distributed dark matter. But Milgrom can't specify a physical mechanism.

My thesis:
Since the beginning of the 20. century, **Einstein's gravitational law** is the gold standard, **not Newton's**! According to this, gravitation means curvature of space. Deviations of a straight path provoke an acceleration and thus a radiation of **gravitational waves**. Not only at strong accelerations, i.e. at two black holes orbiting each other, but also at weak accelerations, one can determine deviations from the Newtonian law, because the **Schwarzschild universe** provides a **minimum curvature** and thus a **minimum acceleration**.
Furthermore, one can presume that bigger agglomerations of celestial bodies that are commonly named globular clusters or galaxies, are not steady.
I postulate a permanent shrinking of clusters and galaxies, caused by permanent radiation of gravitational waves. The 'balanced state' of a galaxy is a spheroid, however shrinking. Due to a fly by of a mass-rich object, a galaxy receives angular momentum and forms **two** opposite wings, returning to its balanced state after loosing the angular momentum. The wings of spiral galaxies rotate by no means according to the Keplarian laws, but permanently reduce their distance to the centre of a galaxy. One cannot explain this by friction, i.e. by radiation of electro-magnetic waves at matter, having on average such small density. At the outskirts of galaxies, the local curvature, affected by local masses, superimpose the cosmic minimum curvature of R_U. The changeover function from the local curvature to the cosmic curvature is given by $R_{ges} = \sqrt{R_{lokal}^2 + R_U^2}$, according to the Pythagorean theorem. Thus, one gets a sharp crossover from the Newtonian to the cosmological dynamics at small accelerations. This leads to the multiple observed too high revolution velocities of matter at the outskirts of galaxies.

6.6.2 (Gravitational) External Field Effect

In conjunction with MOND, the **e**xternal **fie**ld **e**ffect (EFE) is discussed. This effect implies that the outer surrounding of a star system influences its inner dynamics, because one can find galaxies, having a low inner velocity dispersion. According to the **standard** model, this is a hint that there needn't to be a halo consisting of dark matter. This is considered to be further evidence for the existence (!) of dark matter in other star systems. For example, the globular clusters of the ultra diffuse elliptical galaxy
NGC 1052-DF2 move extraordinary slowly (refer to →van Dokkum et al. 2018). (→Milgrom 2008, a review paper) ascribes this to an intrinsic acceleration g_e of the outer surrounding, being just smaller than Milgrom's a_0 , and therefore he can defend his hypothesis.

My thesis:
In the **Schwarzschild universe**, the external field effect can be explained without additional assumptions: As indicated in chapter 3.4, the gradually clumping of the universe's matter provokes that the pristine space curvature becomes unsteady. But the whole curvature remains on average constant. So there have to be areas with higher curvature (i.e. filaments) and areas with a curvature of nearly zero (i.e. voids).Even at local scopes, the depletion of matter effects that the curved space approximates to the euclidean space; the geometry gets partly flat. Thus, the patterns of movement of the embedded objects follow the classical mechanics.
According to this, the absence of gravity inside of a gigantic 3-dimensional hollow sphere is an 'external field effect', on the contrary to the common gravitation at its outside. To this subject, there are intersections to chapter 6.2.16 (low surface brightness galaxies).

For illustration:
A classical soccer ball is composed of 12 pentagons and 20 hexagons. The corresponding multi-angular body is named truncated icosahedron. Just due to stretchability and bendability of the components, the body approximates a perfect globe by strongly pumping up. If the single plains were nearly rigid and inelastic, their curvature were nearly zero, whereas the corners and ridges were above-averaged curved. So one gets a simple 3-dimensional model of the 4-dimensional universe with voids and filaments.

6.6.3 Anomaly of Motion of Spacecrafts

1. A flyby (or swing-by) manoeuvre serves as a global enhancement of a spacecraft by means of one or more near transits to planets. Thereafter, the spacecraft flies nearly solely under the decreasing gravitational field of the sun, if it is on the way to the outskirts of the solar system. From the point of view of the planet being transited, it is expected that the hyperbolic initial velocity is equal to the end velocity (= speed at infinity). But this wasn't the case at a flyby operation of the Galileo spacecraft around the earth. The speed at infinity (~8.95 km/s) was increased by ~4 mm/h (refer to →Turyshew & Toth 2009). This effect is confirmed for many

different spacecrafts passing different planets. Turyshew & Toth couldn't explain this physical effect.
2. At the Pioneer-10 spacecraft, (⟶Anderson et al. 2001) determine an radial additional acceleration of $8.73 \pm 1.33 \cdot 10^{-10} ms^{-2}$ towards the sun over a period of 11.5 years (from January 1987 to July 1998), provoking a reduction of the speed of $0.32 ms^{-1}$. The spacecraft had left the solar system at 1983. (⟶Turyshev et al. 2012) calculate a model of the spacecraft, ascribing the additional deceleration to asymmetric radiation of electro-magnetic energy, however with an error bar of 20%, thus to normal physics.

My thesis:
1. Mercury radiates **gravitational waves** at its orbital movements that leads to the perihelion precession, just as well as at twin-pulsars (chapter 4.3). In both cases, the distance to the counterpart decreases, affecting the additional **acceleration** of the orbital velocity. The flyby of a spacecraft to a planet with hyperbolic velocity, can be considered as one single *incomplete* orbit. The loss of kinetic energy by gravitational waves is overcompensated by the approach to the central body; it 'skids down' a little bit into the local potential funnel of the central body. So the spacecraft becomes faster than assumed according to the Newtonian laws.
2. Travelling in the 'empty' space, respectively radial away from the sun, the spacecraft moves 'on' the radius of the *cosmos*, respectively 'on' the local surface of the potential funnel of the *sun*, and it cannot approach further to the centre of gravity of the *cosmos*. In this case, the loss of energy affects a **deceleration** of the spacecraft. This (negative) additional acceleration corresponds rather exactly to Milgrom's a_0 (chapter 6.6.1), and it is an analogy to the **cosmologic redshift.**

A comment:
To provide evidence for anomalies of motion, one should build a spacecraft of feasible approximated spherical-symmetrical form, even at the inner composition. Per example, the outer shape could be a regular dodecahedron. On many plains, antennas and, if necessary, control nozzles should be regularly distributed. All transmitting antennas should broadcast simultaneously, not only the antenna pointing to the receiver, because even the radio waves operate like a propulsion.
To reduce the technical effort, in particular the power of transmission, one little spacecraft could fly ahead to a main spacecraft for a few hours, serving as a relay station.

7 Conclusions

Cosmologists are proud that the actual valid standard model of cosmology gets along with 'only six parameters', as described by (→Rees 2001) in his book. However, at that time the parameter Ω_Λ for dark energy had been established. Beside this 6 primordial parameters of the Bardeen-Lemaitre universe ($H_0, \Omega_B, \Omega_{CDM}, A_S, n_S, \tau$), (→Tegmark et al. 2005) list 11 further parameters. By the way, the particle physics has 26 additional parameters. Therein (→Smolin 2006) sees a problem: With at least 17 parameters of cosmology, serving mainly for computer simulations, one can simulate evolutions of any kind ('precision cosmology'). Copernicus had comparable problems with his heliocentric world view that was initially quantitatively in an inferior position to the epicycle model. By adding more and more parameters to the geocentric model, the epicycle model described the observations much more accurately, because Copernicus adhered to perfect circular orbits. Kepler revised this afterwards.
In the **Schwarzschild universe**, just **one parameter** leaves to determine, i.e. the Schwarzschild radius R_S , only depending on the three fundamental physical constants, described in equation 11. R_S can be named Hubble radius just as well.

My summary:
The philosophical principle of falsifiability and the sparingness of fundamental assumptions in scientific theories may not play a major role in workaday researches of scientists. This paper merely can be understood as a invitation, to concern oneself with the basement of cosmology, being installed at the beginning of the 20th century and being partly forgotten after the second world war. The herein launched model of the **Schwarzschild universe** is only a raw concept with primary quantitative shortcomings.

There is no excuse the community not to deal with alternative cosmic models any more !

List of Literature

Alavi, A. et al. 2014: '*Ultra-faint Ultraviolet Galaxies at z~2 Behind the Lensing Cluster Abell 1689: the Luminosity Function, Dust Extinction and Star Formation Rate Density*' (https://arxiv.org/abs/1305.2413)

Anderson, J. D. et al. 2001: '*Study of the anomalous acceleration of Pioneer 10 and 11*' (https://arxiv.org/abs/gr-qc/0104064)

Arnouts, S. et al. 2005: '*The GALEX-VVDS Measurement of the Evolution of the 1500A Luminosity Function*' (https://arxiv.org/abs/astro-ph/0411391)

Atek, H. et al. 2014: '*Probing the z>6 Universe with the first Hubble Frontier Fields cluster Abell 2744*' (https://arxiv.org/abs/1311.7670)

Babock, H. W., 1939: '*The Rotation of the Andromeda Nebula*', LicOB 498, 41 (https://articles.adsabs.harvard.edu/full/1939LicOB..19...41B)

Barth, Aaron J., 2007: '*A Normal Stellar Disk in the Galaxy Malin 1*', AJ 133, (https://ui.adsabs.harvard.edu/abs/2007AJ....133.1085B/abstract)

Bertotti, B. Iess, L. & Tortora, P., 2003: '*A test of general relativity using radio links with the Cassini spacecraft*', Nature 425, 374 (https://www.nature.com/articles/nature01997)

Boksenberg, A. et al., 1977: '*The remarkable Seyfert galaxy Markarian 231*', MNRAS 178, 451 (https://ui.adsabs.harvard.edu/abs/1977MNRAS.178..451B/abstract)

Bothun, G. D. et al. , 1987: '*DISCOVERY OF A HUGE LOW-SURFACE-BRIGHTNESS GALAXY*', 94, 23 (https://ui.adsabs.harvard.edu/abs/1987AJ.....94...23B/abstract)

Bouwens, R. J. et al. 2007: '*UV Luminosity Functions at z~4, 5, and 6 from the HUDF and other Deep HST ACS Fields: Evolution and Star Formation History*' (https://arxiv.org/abs/0707.2080)

Bouwens, R. J. et al. 2011: '*UV Luminosity Functions from 132 z~7 and z~8 Lyman-Break Galaxies in the ultra-deep HUDF09 and wide-area ERS WFC3/IR Observations*' (https://arxiv.org/abs/1006.4360)

Bouwens, R. J. et al. 2014: '*UV-Continuum Slopes of >4000 z~4-8 Galaxies from the HUDF/XDF, HUDF09, ERS, CANDELS-South, and CANDELS-North Fields*' (https://arxiv.org/abs/1306.2950)

Bowler R. A. A. et al. 2014: '*The bright end of the galaxy luminosity function at z ~ 7: before the onset of mass quenching?*' (https://arxiv.org/abs/1312.5643)

Braedley, L. D. et al. 2012: '*The Brightest of Reionizing Galaxies Survey: Constraints on the Bright End of the z~8 Luminosity Function*' (https://arxiv.org/abs/1204.3641)

Bruzual, A. G., & Charlot, S., 1993: '*Spectral Evolution of Stellar Populations Using Isochrone Synthesis*', ApJ 405, 538 (https://ui.adsabs.harvard.edu/abs/1993ApJ...405..538B/abstract)

Cardone, V.F. & Cantiello, M., 2003: '*Pixel lensing observations towards globular clusters*', A&A 405, 125 (https://www.aanda.org/articles/aa/abs/2003/25/aah4153/aah4153.html)

Carroll, S. M. 2001: '*The Cosmological Constant*' (https://link.springer.com/article/10.12942/lrr-2001-1)

Crawford, D. F. 2009: '*Observations of type 1a supernovae are consistent with a static universe*' (https://arxiv.org/abs/0901.4172)

de Boer, Willem 2004: Script '*Einführung in die Kosmologie*', Karlsruhe Institute of Technology (https://docplayer.org/40981108-In-die-kosmologie-prof-dr-w-de-boer.html)

Dekel, Avishai 1994: '*Dynamics of Cosmic Flows*' (https://arxiv.org/abs/astro-ph/9401022)

Demarco, R. 2003: '*A study of dark matter halos and gas properties in clusters of galaxies from ROSAT data*' (https://arxiv.org/abs/astro-ph/0306081)

Eddigton, A. S. 1920: '*Space Time and Gravitation*', Cambridge University Press, Reprint edition, ISBN: 978-0521337090

Eddington, A. S., 1930: '*On the Instability of Einstein's Spherical World*', MNRAS 90.7, 668 (https://academic.oup.com/mnras/article-pdf/90/7/668/2901975/mnras90-0668.pdf)

Einstein, Albert, 1915: '*Erklärung der Perihelbewegung des Merkur aus der allgemeinen Relativitätstheorie*', SPAW 1915, 831 (https://ui.adsabs.harvard.edu/abs/1915SPAW.....831E/abstract)

Einstein, Albert, 1916: '*Näherungsweise Integration der Feldgleichungen der Gravitation*', SPAW 1916, 688 (https://ui.adsabs.harvard.edu/abs/1916SPAW.....688E/abstract)

Einstein, Albert, 1917: '*Kosmologische Betrachtungen zur allgemeinen Relativitätstheorie*', SPAW 1917, 142 (https://ui.adsabs.harvard.edu/abs/1917SPAW.....142E/abstract)

Einstein, Albert, 1918: '*Über Gravitationswellen*', SPAW 1918, 154 (https://ui.adsabs.harvard.edu/abs/1918SPAW.....154E/abstract)

Fan, L. et al. 2016: '*Infrared spectral energy distribution decomposition of WISE-selected, hyperluminous hot dust-obscured galaxies*' (https://arxiv.org/abs/1604.01467)

Fan, X. et al., 2001: '*A Survey of z > 5.8 Quasars in the Sloan Digital Sky Survey I*', AJ 122, 2833 (https://iopscience.iop.org/article/10.1086/324111)

Finkelstein, S. L. et al. 2014: '*The Evolution of the Galaxy Rest-Frame Ultraviolet Luminosity Function Over the First Two Billion Years*' (https://arxiv.org/abs/1410.5439)

Gamow, G., 1948: '*The Evolution of the Universe*', Nature 162, 680 (https://www.nature.com/articles/162680a0)

Genzel, R. & Cesarsky, C. J. 2000: '*Extragalactic Results from the Infrared Space Observatory*' (https://arxiv.org/abs/astro-ph/0002184)

Gilfanov, M. & Bogdan, A. 2010: '*An upper limit on the contribution of accreting white dwarfs to the type Ia supernova rate*' (https://arxiv.org/abs/1002.3359)

Golimowski, D. A., 2004: '*L' and M' Photometry of Ultracool Dwarfs*', AJ 127, 3516 (https://ui.adsabs.harvard.edu/abs/2004AJ....127.3516G/abstract)

Groom, D. E. & Scott, D. 2019: '*Astrophysical Constants and Parameters*' (http://pdg.lbl.gov/2019/reviews/rpp2019-rev-astrophysical-constants.pdf)

Guth, Alan H., 1981: '*Inflationary universe: A possible solution to the horizon and flatness problems*', PhysRev D 23, 347 (https://journals.aps.org/prd/abstract/10.1103/PhysRevD.23.347)

Hathi, N. P. et al 2010: '*UV-dropout Galaxies in the GOODS-South Field from WFC3 Early Release Science Observations*' (https://arxiv.org/abs/1004.5141)

Hennawi, J. F. et al. 2006a: '*Quasars Probing Quasars I: Optically Thick Absorbers Near Luminous Quasars*' (https://arxiv.org/abs/astro-ph/0603742)

Hennawi, J. F. et al. 2006b: '*Quasars Probing Quasars II: The Anisotropic Clustering of Optically Thick Absorbers around Quasars*' (https://arxiv.org/abs/astro-ph/0606084)

Hogg, D. W. 1999: '*Distance measures in cosmology*' (https://arxiv.org/abs/astro-ph/9905116)

Hubble, E., Humason, M. L., 1931: '*The Velocity-Distance Relation among Extra-Galactic Nebulae*', ApJ , 43 (https://ui.adsabs.harvard.edu/abs/1931ApJ....74...43H/abstract)

Hubble, E., Humason, M. L., : '*The Law of Red-shifts*', MNRAS 113, 658 (https://academic.oup.com/mnras/article-pdf/113/6/658/9073577/mnras113-0658.pdf)

Ishigaki, M. et al. 2014: '*Hubble Frontier Fields First Complete Cluster Data: Faint Galaxies at z~5 - 10 for UV Luminosity Functions and Cosmic Reionization*' (https://arxiv.org/abs/1408.6903)

Jee, Inh, 2019: '*A measurement of the Hubble constant from angulardiameter distances to two gravitational lenses*', , (https://arxiv.org/abs/1909.06712)

Jha, S., Riess, A., Kirschner, R.P., 2007: '*Improved Distances to Type Ia Supernovae with Multicolor Light-Curve Shapes: MLCS2k2*', ApJ 659, 122 (https://ui.adsabs.harvard.edu/abs/2007ApJ...659..122J/abstract)

Kim, D.-C., 1995: '*Optical Spectroscopy of Luminous Infrared Galaxies. I. Nuclear Data*', ApJS 98, 129 (https://ui.adsabs.harvard.edu/abs/1995ApJS...98..129K/abstract)

Kowalski, M. 2008: '*Improved Cosmological Constraints from New, Old and Combined Supernova Datasets*' (https://arxiv.org/abs/0804.4142)

Léger, A., Puget, J. L., 1984: '*Identification of the Unidentified Infrared Emission Features of Interstellar Dust* ', A&A 137, 5L (https://ui.adsabs.harvard.edu/abs/1984A%26A...137L...5L/abstract)

Leighley, Karen M. 2016: '*The Binary Black Hole Model for Mrk 231 Bites the Dust*' (https://arxiv.org/abs/1604.03456)

Lerner, E. J. 2018: '*Observations contradict galaxy size and surface brightness predictions that are based on the expanding universe hypothesis*' (https://arxiv.org/abs/1803.08382)

Lerner, E. J. , Falomo, R. , Scarpa, R. 2014: '*UV surface brightness of galaxiesfrom the local Universe to z ~ 5*' (https://arxiv.org/abs/1405.0275)

Lewis, G. F. & Brewer, B. J. 2023: '*Detection of the Cosmological Time Dilation of High Redshift Quasars*' (https://arxiv.org/abs/2306.04053)

Lilly, S. J. 1996: '*The CANADA-FRANCE REDSHIFT SURVEY XIII: The luminosity density and star-formation history of the Universe to z ~ 1*' (https://arxiv.org/abs/astro-ph/9601050)

Linde, A. 1995: '*Quantum Cosmology and the Structure of Inflationary Universe*' (https://arxiv.org/abs/gr-qc/9508019)

Little, B. & Weinberg, D. H. 1993: '*Cosmic Voids and Biased Galaxy Formation*' (https://arxiv.org/abs/astro-ph/9306006)

Lubin, L. M., Sandage, A. 2001a: '*The Tolman Surface Brightness Test for the Reality of the Expansion. II. The Effect of the Point-Spread Function and Galaxy Ellipticity on the Derived Photometric Parameters* ' (https://arxiv.org/abs/astro-ph/0102214)

Lubin, L. M., Sandage, A. 2001b: '*The Tolman Surface Brightness Test for the Reality of the Expansion. III. HST Profile and Surface Brightness Data for Early-Type Galaxies in Three High-Redshift Clusters*' (https://arxiv.org/abs/astro-ph/0106563)

Lubin, L. M., Sandage, A. 2001c: '*The Tolman Surface Brightness Test for the Reality of the Expansion. IV. A Measurement of the Tolman Signal and the Luminosity Evolution of Early-Type Galaxies*' (https://arxiv.org/abs/astro-ph/0106566)

McLure, R. J. et al. 2009: '*The luminosity function, halo masses and stellar masses of luminous Lyman-break galaxies at redshifts 5<z<6*' (https://arxiv.org/abs/0805.1335)

McLure, R. J. et al. 2013: '*A new multi-field determination of the galaxy luminosity function at z=7-9 incorporating the 2012 Hubble Ultra Deep Field imaging*' (https://arxiv.org/abs/1212.5222)

Milgrom, M., 1983a: '*A modification of the Newtonian dynamics as a possible alternative to the hidden mass hypothesis*', ApJ 270, 365 (https://ui.adsabs.harvard.edu/abs/1983ApJ...270..365M/abstract)

Milgrom, M., 1983b: '*A modification of the Newtonian dynamics - Implications for galaxies*', ApJ 270, 371 (https://ui.adsabs.harvard.edu/abs/1983ApJ...270..371M/abstract)

Milgrom, M. 2008: '*The MOND paradigm*' (https://arxiv.org/abs/0801.3133)

Mo, H. J., Mao, S., White, S. D. M., 1998: '*The formation of galactic discs*', MNRAS 295, 319 (https://academic.oup.com/mnras/article/295/2/319/987489)

Oesch P. A. et al. 2007: '*The UDF05 Follow-up of the HUDF: I. The Faint-End Slope of the Lyman-Break Galaxy Population at z~5*' (https://arxiv.org/abs/0706.2653)

Oesch, P. A. et al. 2010: '*The Evolution of the UV Luminosity Function from z ~ 0.75 to z ~ 2.5 using HST ERS WFC3/UVIS Observations*' (https://arxiv.org/abs/1005.1661)

Onken, C. A. 2021: '*Ultra-luminous high-redshift quasars from SkyMapper II*' (https://arxiv.org/abs/2105.12215)

Ouchi, M. et al. 2009: '*Large Area Survey for z=7 Galaxies in SDF and GOODS-N: Implications for Galaxy Formation and Cosmic Reionization*' (https://arxiv.org/abs/0908.3191)

Parsa, S. et al. 2015: '*The galaxy UV luminosity function at z ~ 2 - 4; new results on faint-end slope and the evolution of luminosity density*' (https://arxiv.org/abs/1507.05629)

Penzias, A.A. & Wilson, R. W., 1965: '*A Measurement of Excess Antenna Temperature at 4080 Mc/s.*', AJ 142, 419 (https://ui.adsabs.harvard.edu/abs/1965ApJ...142..419P/abstract)

Perlmutter, S. 1998: '*Measurements of Ω and Λ from 42 High-Redshift Supernovae*' (https://arxiv.org/abs/astro-ph/9812133)

Peters, P. C. & Mathews, J., 1963: '*Gravitational Radiation from Point Masses in a Keplerian Orbit*', PhyRev , 435 (https://journals.aps.org/pr/abstract/10.1103/PhysRev.131.435)

Phillips, M. M., **1993**: '*The Absolute Magnitudes of Type IA Supernovae*', ApJL 413, 105 (https://ui.adsabs.harvard.edu/abs/1993ApJ...413L.105P/abstract)

Planck Collaboration, **2014**: '*Planck 2013 results. XVI. Cosmological parameters*', A&A 571, Part 16 (https://ui.adsabs.harvard.edu/abs/2014A%26A...571A..16P/abstract)

Powell, Richard 2000: '*cosmodis - A Cosmological Distances Program - version 1.1*' (http://www.atlasoftheuniverse.com/cosmodis.c)

Puget, J. L., Léger, A., **1989**: '*A new component of the interstellar matter - Small grains and large aromatic molecules*', ARA&A 27, 161 (https://adsabs.harvard.edu/full/1989ARA%26A..27..161P)

Reddy, N. A. & Steidel, C.C. 2009: '*A Steep Faint-End Slope of the UV Luminosity Function at z~2-3: Implications for the Global Stellar Mass Density and Star Formation in Low Mass Halos*' (https://arxiv.org/abs/0810.2788)

Rees, Martin 2001: '*Just Six Numbers: The Deep Forces That Shape the Universe*', Basic Books, , ISBN: 9780465036738

Riess, A. G. et al., **1998**: '*Observational Evidence from Supernovae for an Accelerating Universe and a Cosmological Constant*', AJ 116, 1009 (https://ui.adsabs.harvard.edu/abs/1998AJ....116.1009R/abstract)

Rosenbaum, S.D. et al., **2007**: '*The large-scale environment of low surface brightness galaxies*', A&A 504, 807 (https://www.aanda.org/articles/aa/pdf/2009/36/aa7462-07.pdf)

Rubin, V. & Fort, K., **1970**: '*ROTATION OF THE ANDROMEDA NEBULA FROM A SPECTROSCOPIC SURVEY OF EMISSION REGIONS*', ApJ 159, 379 (https://ui.adsabs.harvard.edu/abs/1970ApJ...159..379R/abstract)

Rubin, V. et al., **1978**: '*EXTENDED ROTATION CURVES OF HIGH-LUMINOSITY SPIRAL GALAXIES IV*', ApJL 225, 107 (https://ui.adsabs.harvard.edu/abs/1978ApJ...225L.107R/abstract)

Sandage, A. 2009: '*The Tolman Surface Brightness Test for the Reality of the Expansion. V. Provenance of the Test and a New Representation of the Data for Three Remote HST Galaxy Clusters*' (https://arxiv.org/abs/0905.3199)

Sandage, A., Lubin, L. M. 2001: '*The Tolman Surface Brightness Test for the Reality of the Expansion. I. Calibration of the Necessary Local Parameters*' (https://arxiv.org/abs/astro-ph/0102213)

Sawicki, M. 2012: '*Stars, Dust, and the Growth of UV-Selected Sub-L* Galaxies at Redshift z~2*' (https://arxiv.org/abs/1108.5186)

Sawicki, M. and Thompson, D. 2006: '*Keck Deep Fields. III. Luminosity-dependent Evolution of the Ultraviolet Luminosity and Star Formation Rate Densities at z~4, 3, and 2*' (https://arxiv.org/abs/astro-ph/0605406)

Schechter, P. L., **1976**: '*An analytic expression for the luminosity function for galaxies*', ApJ 203, 297 (https://ui.adsabs.harvard.edu/abs/1976ApJ...203..297S/abstract)

Schenker, M. A. et al. 2013: '*The UV Luminosity Function of star-forming galaxies via dropout selection at redshifts z ~ 7 and 8 from the 2012 Ultra Deep Field campaign*' (https://arxiv.org/abs/1212.4819)

Schmidt, K. B. et al. 2014: '*The Luminosity Function at z~8 from 97 Y-band dropouts: Inferences About Reionization*' (https://arxiv.org/abs/1402.4129)

Schneider, Peter 2008: '*Extragalactic Astronomy and Cosmology*', Springer, , ISBN: 3-540-33174-3

Schwarzschild, Karl, **1916**: '*Über das Gravitationsfeld eines Massenpunktes nach der Einsteinschen Theorie*', SPAW 1916, 189 (https://ui.adsabs.harvard.edu/abs/1916SPAW.....189S/abstract)

Shapiro , I. I., **1964**: '*Fourth Test of General Relativity*', Phys. Rev. Lett. 13, 789 (https://journals.aps.org/prl/abstract/10.1103/PhysRevLett.13.789)

Shapiro , I. I. et al., **1968**: '*Fourth Test of General Relativity: Preliminary Results*', Phys. Rev. Lett. 20, 1265 (https://journals.aps.org/prl/abstract/10.1103/PhysRevLett.20.1265)

Smolin, Lee 2006: '*The Trouble with Physics*', Houghton Mifflin Harcourt, , ISBN: 978-0-618-55105-7

Soifer, B. T., Houck, J. R., Neugebauer, G., **1987**: '*The IRAS View of the Extragalactic Sky*', ARA&A , (https://adsabs.harvard.edu/full/1987ARA%26A..25..187S)

Springel, V. 2005: '*Simulating the joint evolution of quasars, galaxies and their large-scale distribution*' (https://arxiv.org/abs/astro-ph/0504097)

Tegmark, Max et al. 2005: '*Dimensionless constants, cosmology and other dark matters* ' (https://arxiv.org/pdf/astro-ph/0511774)

The LIGO Collaboration 2019: '*Tests of General Relativity with the Binary Black Hole Signals from the LIGO-Virgo Catalog GWTC-1*' (https://arxiv.org/abs/1903.04467)

Tolman, R.C., **1930**: '*On the Estimation of Distances in a Curved Universe with a Non-Static Line Element*', Proc.N.A.S. 16, 511 (https://www.pnas.org/doi/abs/10.1073/pnas.16.7.511)

Turner, M. S., **1999**: '*Dark Matter and Dark Energy in the Universe*', ASP Conference Series 165, 431 (http://www.aspbooks.org/a/volumes/article_details/?paper_id=17135)

Turyshew, S. G. & Toth, V. T. 2009: '*The Puzzle of the Flyby Anomaly*' (https://arxiv.org/abs/0907.4184)

Turyshew, S. G. et al. 2012: '*Support for the thermal origin of the Pioneer anomaly*' (https://arxiv.org/abs/1204.2507)

van der Burg, R.F. J., Hildebrand, H., Erben, T. 2010: '*The UV galaxy luminosity function at z=3-5 from the CFHT Legacy Survey Deep fields*' (https://arxiv.org/abs/1009.0758)

van Dokkum, P. 2018: '*A galaxy lacking dark matter*' (https://arxiv.org/abs/1803.10237)

Weisberg, J. M., Nice, D. J., Taylor, J. H. 2010: '*Timing Measurements of the Relativistic Binary Pulsar PSR B1913+16*' (https://arxiv.org/abs/1011.0718)

Weisz, D. R. et al. 2014: '*The Very Faint End of the UV Luminosity Function over Cosmic Time: Constraints from the Local Group Fossil Record*' (https://arxiv.org/abs/1409.4772)

Weizsäcker, Carl Friedrich : zitiert von Ernst Peter Fischer in Mannheimer Forum 92/93, Seite112

Weyder T. K. et al. 2005: '*The UV Galaxy Luminosity Function in the Local Universe from GALEX Data*' (https://arxiv.org/abs/astro-ph/0411364)

Yoshida, M. et al. 2006: '*Luminosity Functions of Lyman-Break Galaxies at z~4 and 5 in the Subaru Deep Field*' (https://arxiv.org/abs/astro-ph/0608512)

Zwicky, F., 1929: '*ON THE REDSHIFT OF SPECTRAL LINES THROUGH INTERSTELLAR SPACE*', PNAS 15, 773 (https://www.ncbi.nlm.nih.gov/pmc/articles/PMC522555/)

Zwicky, F., 1933: '*Die Rotverschiebung von extragalaktischen Nebeln*', AcHPh 6, 110 (https://ui.adsabs.harvard.edu/abs/1933AcHPh...6..110Z/abstract)

Zwicky, F., 1937: '*On the Masses of Nebulae and of Clusters of Nebulae*', ApJ 86, 217 (https://ui.adsabs.harvard.edu/abs/1937ApJ....86..217Z/abstract)